PHARMACIA

Pharmacia 73: 1–22
DOI 10.3897/pharmacia.73.e173385

Research Article

# Design and *in silico* study of thiourea–pyrazolopyrimidine hybrids as dual PI3K/mTOR inhibitors for cancer therapy

Ruswanto Ruswanto[1], Tita Nofianti[1], Richa Mardaningrum[2], Dini Kesuma[3], Sofa Fajriah[4], Aska Reisya Aulia[1], Sheilla Fitriani Zahwa[1], Zahra Putri Handirana[1]

1 *Pharmacy Program, Universitas Bakti Tunas Husada, Tasikmalaya 46115, West Java, Indonesia*
2 *Pharmacy Program, Faculty of Health Science, Universitas Perjuangan, Tasikmalaya 46115, West Java, Indonesia*
3 *Pharmacy Program, Faculty of Pharmacy, Universitas Surabaya, Surabaya 60293, East Java, Indonesia*
4 *Research Center for Pharmaceutical Ingredients and Traditional Medicine, National Research and Innovation Agency (BRIN), Kawasan Sains Teknologi Dr. (H.C) Ir. H. Soekarno, Jl. Raya Bogor KM. 46, Cibinong 16911, Indonesia*

Corresponding author: Ruswanto Ruswanto (ruswanto@universitas-bth.ac.id)

**Received** 28 September 2025 ♦ **Accepted** 18 January 2026 ♦ **Published** 2 February 2026

**Citation:** Ruswanto R, Nofianti T, Mardaningrum R, Kesuma D, Fajriah S, Aulia AR, Zahwa SF, Handirana ZP (2026) Design and *in silico* study of thiourea–pyrazolopyrimidine hybrids as dual PI3K/mTOR inhibitors for cancer therapy. Pharmacia 73: 1–22. https://doi.org/10.3897/pharmacia.73.e173385

## Abstract

**Background:** Cancer remains a major cause of mortality worldwide, with the PI3K/mTOR signaling pathway playing a crucial role in tumor progression, proliferation, and therapeutic resistance. Although several dual PI3K/mTOR inhibitors have been developed, their clinical outcomes remain limited due to poor bioavailability, significant toxicities, and rapid resistance. Molecular hybridization offers a rational strategy to address these limitations by integrating multiple pharmacophores into a single scaffold.

**Aim:** This study aimed to design and evaluate thiourea–pyrazolopyrimidine hybrids as potential dual PI3K/mTOR inhibitors using *in silico* approaches, supported by the preliminary synthesis of precursor molecules.

**Materials and methods:** Eighty hybrid compounds were generated using ChemDraw and MarvinSketch, optimized by energy minimization, and docked against PI3K (PDB ID: 3L54) and mTOR (PDB ID: 4JT6) using AutoDock 4.2. The best candidates were further validated through 30 ns molecular dynamics (MD) simulations using Desmond, while pharmacokinetic and toxicity properties were assessed using pkCSM.

**Results:** Several derivatives, particularly 2-phenylbenzoate and 4-thiophen analogs, demonstrated stronger binding affinities than native ligands, supported by stable hydrogen bonding and hydrophobic interactions. MD simulations confirmed the stability of the complexes, with RMSD and RMSF values indicating consistent conformations throughout the trajectory. ADMET predictions suggested favorable absorption, low CYP450 inhibition, and reduced mutagenic potential, especially for $CF_3$ and lipophilic substituents.

**Conclusion:** In conclusion, thiourea–pyrazolopyrimidine hybrids exhibit promising dual PI3K/mTOR inhibitory potential with enhanced pharmacokinetic and safety profiles compared to lead compounds. These results establish a solid foundation for further synthesis, characterization, and biological evaluation as novel anticancer candidates.

## Keywords

Anticancer, dual PI3K/mTOR inhibitor, *in silico*, synthesis, thiourea–pyrazolopyrimidine hybrids

## Introduction

Cancer remains one of the leading causes of mortality worldwide, with incidence rates continuing to rise each year. Recent global statistics underscore its critical impact, positioning cancer as one of the most pressing public health challenges of the 21st century (Siegel et al. 2023). Among the key signaling pathways implicated in tumor progression, the phosphatidylinositol 3-kinase/mammalian target of rapamycin (PI3K/mTOR) axis plays a central role in regulating cell growth, proliferation, metabolism, and survival. Dysregulation of this pathway is strongly associated with tumorigenesis and the emergence of resistance to conventional therapies (Porta et al. 2014; Janku et al. 2018).

Over the past decade, several PI3K/mTOR inhibitors have been developed, including BEZ235 (dactolisib), GDC-0980, and PF-04691502, which initially demonstrated promising dual-target activity. However, these agents are limited by poor bioavailability, dose-limiting toxicities, and the rapid emergence of drug resistance, significantly hampering their clinical utility (Sabbah et al. 2011; Janku et al. 2018; Gao et al. 2023). Consequently, multi-target inhibition strategies are increasingly recognized as more effective therapeutic approaches than single-target inhibition, offering the potential for improved selectivity, reduced toxicity, and enhanced metabolic stability (Kucuksayan and Ozben 2017; Gontijo et al. 2020, 2020; Szumilak et al. 2021; Wang and Tortorella 2022).

In this context, thiourea derivatives have emerged as a class of compounds with notable anticancer potential. Several 1-benzoyl-3-methylthiourea derivatives have been synthesized and reported to induce apoptosis, inhibit cancer cell proliferation, and modulate oncogenic signaling pathways, although their therapeutic application remains constrained by poor selectivity and cytotoxicity (Ruswanto and Siswandono 2015; Ruswanto et al. 2017, 2018, 2021, 2023a). In contrast, pyrazolopyrimidines represent a privileged heterocyclic scaffold with a well-documented affinity for the ATP-binding domain of PI3K/mTOR, making them attractive structural motifs for inhibitor design (Sabbah et al. 2011; Lee et al. 2013; Welker and Kulik 2013).

A rational approach to overcome these limitations is molecular hybridization, which involves the integration of two pharmacophores into a single hybrid entity. This strategy has been successfully applied in the design of multi-target drug candidates, yielding molecules with synergistic biological effects, improved pharmacokinetic properties, and reduced resistance profiles compared to single agents (Kucuksayan and Ozben 2017; Gontijo et al. 2020; Szumilak et al. 2021). Accordingly, the development of thiourea–pyrazolopyrimidine hybrids holds considerable promise, as such molecules may combine the anticancer potential of thioureas with the high affinity of pyrazolopyrimidines toward PI3K/mTOR, thereby enhancing hydrophobic interactions, binding affinity, and metabolic stability while reducing toxicity (Lee et al. 2013; Huang et al. 2022).

To rationalize this drug design, *in silico* approaches provide a powerful and cost-effective strategy. Computational methods such as molecular docking are widely employed to evaluate ligand–protein binding affinities (Jain and Gupta 2023), while molecular dynamics (MD) simulations allow for the assessment of the stability of ligand–target complexes under physiological conditions (Ruswanto et al. 2023b). In addition, *in silico* pharmacokinetic and toxicity predictions (ADMET) serve as essential preliminary filters in early drug discovery, providing valuable insights into drug-likeness and safety profiles (Pires et al. 2015). Collectively, these approaches support the rational design and virtual evaluation of novel thiourea–pyrazolopyrimidine hybrids as potential dual PI3K/mTOR inhibitors for the treatment of cancer.

The novelty of this study lies in the rational hybridization of thiourea and pyrazolopyrimidine pharmacophores into a single molecular scaffold specifically optimized for dual PI3K/mTOR inhibition. Unlike previously reported single-scaffold or loosely related analogs, the proposed hybrids demonstrate enhanced binding affinity, improved interaction stability, and more favorable predicted pharmacokinetic profiles. Notably, several top-ranked hybrids exhibited superior binding free energy and stability compared to reference ligands while maintaining acceptable ADMET characteristics. These findings highlight the advantage of the hybrid design strategy in overcoming limitations associated with earlier PI3K/mTOR inhibitors and underscore the potential of thiourea–pyrazolopyrimidine hybrids as a distinct and promising class of anticancer candidates.

## Materials and methods

### Ligand preparation

Hybrid thiourea–pyrazolopyrimidine derivatives were designed using ChemDraw Ultra 20.0 and subsequently converted into three-dimensional structures. The geometry of each ligand was optimized using MarvinSketch 21.13, employing the MMFF94 force field until energy minimization was achieved. The minimized ligands were then saved in PDBQT format for docking simulations.

### Protein preparation

The three-dimensional crystal structures of PI3K (PDB ID: 3L54) and mTOR (PDB ID: 4JT6) were retrieved from the Protein Data Bank (RCSB PDB). Protein preparation was carried out using AutoDockTools 1.5.7 by removing crystallographic water molecules, heteroatoms, and co-crystallized ligands, followed by the addition of polar hydrogen atoms and assignment of Kollman charges. The processed receptor structures were stored in PDBQT format.

Molecular docking was performed using AutoDock 4.2 with the Lamarckian Genetic Algorithm (LGA) as the search strategy. The docking grid was positioned at the

ATP-binding site of each receptor, with the grid box size adjusted to fully encompass the binding pocket (PI3K: center_x = 13.751, center_y = –4.126, center_z = 22.894; mTOR: center_x = 52.217, center_y = 31.844, center_z = 64.038; grid dimensions = 40 × 40 × 40 Å). Docking parameters included 100 runs, a population size of 150, a maximum of $2.5 \times 10^6$ energy evaluations, and 27,000 generations. Docking results were evaluated based on binding affinity (kcal/mol) and ligand–protein interactions such as hydrogen bonds, hydrophobic contacts, and π–π stacking. Both two- and three-dimensional interaction analyses were conducted using Discovery Studio Visualizer 2021 (Mardianingrum et al. 2021; Ruswanto et al. 2021).

## Molecular dynamics (MD) simulation

The most promising complexes obtained from docking were further subjected to molecular dynamics (MD) simulations using Desmond (Schrödinger Release 2021, Academic Free License) with the OPLS_2005 force field. Each protein–ligand complex was solvated in an orthorhombic simulation box with a 10 Å buffer distance, using the TIP3P water model and 0.15 M NaCl to neutralize the system. Energy minimization was conducted for 100 ps to remove steric clashes, followed by equilibration under the NPT ensemble at 300 K and 1.01325 bar using the Nose–Hoover thermostat and Martyna–Tobias–Klein barostat (Renadi et al. 2023; Septian et al. 2023). Production runs were performed for 30 ns with a 2 fs integration time step, and trajectory frames were recorded every 1.2 ps. Analysis of the MD trajectories was performed using the Simulation Interaction Diagram (SID) tool in Desmond. The parameters assessed included root mean square deviation (RMSD) to monitor overall complex stability, root mean square fluctuation (RMSF) to examine residue flexibility, radius of gyration (rGyr) to assess protein compactness, hydrogen bond occupancy to evaluate interaction stability, and solvent accessible surface area (SASA) to investigate changes in solvent exposure throughout the simulation (Ruswanto et al. 2022, 2023a).

## ADMET prediction

The pharmacokinetic and toxicity profiles of the designed hybrids were predicted using the pkCSM web server. Parameters such as intestinal absorption, blood–brain barrier (BBB) penetration, cytochrome P450 (CYP450) inhibition, mutagenicity (AMES test), and acute toxicity ($LD_{50}$) were evaluated to assess the drug-likeness and safety of the compounds (Pires et al. 2015; Silalahi et al. 2025).

# Results and discussion

Although the present study is limited to *in silico* approaches, it provides a robust and rational framework for the early-stage discovery of dual PI3K/mTOR inhibitors. Computational methods such as molecular docking, molecular dynamics simulations, and ADMET prediction are widely recognized as effective tools for prioritizing lead compounds before costly and time-consuming experimental studies. The identified thiourea–pyrazolopyrimidine hybrids demonstrated favorable binding affinity, stable interactions with key active-site residues, and acceptable predicted pharmacokinetic and safety profiles, supporting their potential as promising lead candidates. Future work will focus on the chemical synthesis of the top-ranked compounds, followed by *in vitro* evaluation against relevant cancer cell lines and subsequent *in vivo* studies to validate their biological activity, mechanism of action, and therapeutic potential.

In this study, 80 hybrid compounds were designed from thiourea derivatives and pyrazolopyrimidine compounds drawn using MarvinSketch 5.2.5.1, with lead compounds shown in Fig. 1.

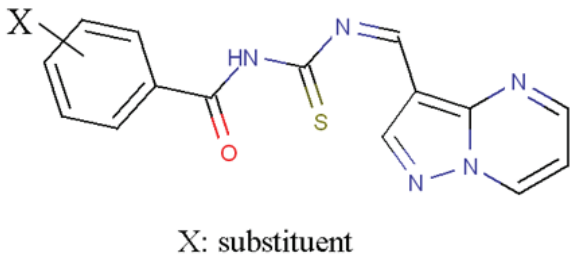


**Figure 1.** Design structure of the proposed hybrid compound.

Before molecular docking and molecular dynamics simulations were performed, the designed compounds were prepared in two stages. First, the ligands were cleaned in 2D format, protonated at physiological blood pH (7.4), and saved in .mrv format. Second, ligand energy minimization was performed, and the structures were saved in .pdb format. Both ligand preparation stages were conducted using MarvinSketch software.

## Pharmacokinetic and toxicity predictions

Pharmacokinetic and toxicity profiles are used in the research and development of new drugs to evaluate the effectiveness and potential side effects of drug candidates and are assessed using https://biosig.lab.uq.edu.au/pkcsm/. This assessment depends on a number of parameters, such as Caco-2, intestinal absorption, VDss, BBB, activity as a substrate and inhibitor of CYP3A4, OCT2, AMES toxicity, hepatotoxicity, and LD50. Tables 1, 2 present the predicted pharmacokinetic and toxicity profiles based on these parameters, providing an overview of the potential performance and risks associated with the test ligands.

Based on the results of pkCSM predictions (Pires et al. 2015), in general, the majority of derivative compounds exhibit fairly good pharmacokinetic profiles. In terms of absorption, most compounds show Caco-2 permeability

**Table 1.** Pharmacokinetic properties of the Cs.

| No. | Substituent | Pharmacokinetic Properties | | | | | |
|---|---|---|---|---|---|---|---|
| | | Absorption | | Distribution | | Metabolism | Excretion |
| | | Caco2 permeability | Intestinal absorption (human) | VDss (human) | BBB permeability | CYP2D6 inhibitor | Renal OCT2 substrate |
| 1 | 4-phenyldiazen | 0.604 | 96.846 | -0.381 | -0.793 | No | No |
| 2 | 4-chloromethyl | 0.997 | 95.328 | -0.536 | -0.688 | No | No |
| 3 | 4-dimethylamino | 1.093 | 97.943 | -0.590 | -0.670 | No | No |
| 4 | 2-chloromethyl | 0.900 | 93.987 | -0.594 | -0.683 | No | No |
| 5 | 3-CF3 | 0.982 | 94.225 | -0.719 | -0.932 | No | No |
| 6 | 3-phenyl acetat | 0.270 | 82.309 | -0.947 | -0.919 | No | No |
| 7 | 4-methylthio | 1.045 | 96.189 | -0.556 | -0.721 | No | No |
| 8 | 2-CF3 | 1.084 | 94.129 | -0.906 | -0.909 | No | No |
| 9 | 3-OCF3 | 1.088 | 93.919 | -1.074 | -1.149 | No | No |
| 10 | 4-trifluoromethylthio | 1.060 | 92.567 | -0.910 | -1.104 | No | No |
| 11 | 4-trifluoromethoxy | 1.088 | 93.919 | -1.074 | -1.149 | No | No |
| 12 | 4-sulfonylchloride | -0.071 | 83.367 | -1.267 | -1.125 | No | No |
| 13 | 4-difluoromethylthio | 1.054 | 93.698 | -0.815 | -0.983 | No | No |
| 14 | 4-difluoromethoxy | 1.082 | 95.050 | -0.979 | -1.028 | No | No |
| 15 | 3,5-CF3 | 1.088 | 90.856 | -1.054 | -1.346 | No | No |
| 16 | 2-F, 5-CF3 | 1.311 | 97.441 | 0.997 | 0.806 | No | No |
| 17 | 2,5-CF3 | 1.088 | 90.856 | -1.054 | -1.346 | No | No |
| 18 | 2-CF3, 4-F | 1.082 | 93.371 | -1.074 | -1.110 | No | No |
| 19 | 2-F, 4-CF3 | 1.082 | 93.371 | -1.074 | -1.110 | No | No |
| 20 | 3-F, 4-CF3 | 1.082 | 93.371 | -1.074 | -1.110 | No | No |
| 21 | 2-F, 3-CF3 | 1.082 | 93.371 | -1.074 | -1.110 | No | No |
| 22 | 2-CF3, 5-F | 1.082 | 93.371 | -1.074 | -1.110 | No | No |
| 23 | 2,4-CF3 | 1.088 | 90.856 | -1.054 | -1.346 | No | No |
| 24 | 2,6-CF3 | 1.088 | 90.856 | -1.054 | -1.346 | No | No |
| 25 | 2-Cl, 4-CF3 | 1.067 | 92.469 | -0.940 | -1.077 | No | No |
| 26 | 3,5-Cl 4-OCH3 | 1.061 | 94.077 | -0.963 | -1.036 | No | No |
| 27 | 2-F, 3-Cl, 5-CF3 | 1.064 | 91.710 | -1.106 | -1.278 | No | No |
| 28 | 2-F, 3-Cl, 6-CF3 | 1.064 | 91.710 | -1.106 | -1.278 | No | No |
| 29 | 3-F, 5-CF3 | 1.311 | 97.441 | 0.997 | 0.806 | No | No |
| 30 | 3-Cl, 6-CF3 | 1.067 | 92.469 | -0.940 | -1.077 | No | No |
| 31 | 4-thiadiazol | 0.204 | 90.665 | -1.299 | -1.073 | No | No |
| 32 | 3-CF3, 4-CH3 | 1.089 | 93.927 | -0.874 | -0.902 | No | No |
| 33 | 4-pyrazol | 1.155 | 97.421 | -1.116 | -0.830 | No | No |
| 34 | 4-bromomethyl | 1.069 | 95.844 | -0.725 | -0.665 | No | No |
| 35 | 2,3,4,5,6-F | 1.068 | 93.609 | -1.551 | -1.476 | No | No |
| 36 | 2-phenylbenzoate | 0.741 | 89.285 | -0.551 | -0.726 | No | No |
| 37 | 4-ethyl | 1.011 | 96.402 | -0.476 | -0.517 | No | No |
| 38 | 2-CN | 0.265 | 85.492 | -0.832 | -0.694 | No | No |
| 39 | 3-CN | 0.265 | 85.492 | -0.832 | -0.694 | No | No |
| 40 | 4-CN | 0.265 | 85.492 | -0.832 | -0.694 | No | No |
| 41 | 4-propyl | 0.991 | 95.675 | -0.354 | -0.483 | No | No |
| 42 | 4-I | 1.061 | 95.714 | -0.658 | -0.747 | No | No |
| 43 | 4-butyl | 0.985 | 95.256 | -0.263 | -0.487 | No | No |
| 44 | 4-heptyl | 0.593 | 94.260 | 0.094 | -0.475 | No | No |
| 45 | 4-hexyl | 0.940 | 94.601 | -0.013 | -0.470 | No | No |
| 46 | 4-octyl | 0.961 | 94.577 | -0.293 | -0.629 | No | No |
| 47 | 4-decyl | 0.943 | 93.739 | -0.164 | -0.677 | No | No |
| 48 | 4-butoxy | 1.087 | 96.142 | -0.704 | -0.772 | No | No |
| 49 | 2,4-CH3 | 1.089 | 96.998 | -0.684 | -0.457 | No | No |
| 50 | 2,4-F | 1.075 | 95.885 | -1.082 | -0.873 | No | No |
| 51 | 3,4-F | 1.075 | 95.885 | -1.082 | -0.873 | No | No |
| 52 | 2,4,6-CH3 | 1.093 | 96.796 | -0.652 | -0.450 | No | No |
| 53 | 2,4,5-F | 1.073 | 95.127 | -1.244 | -1.074 | No | No |

| No. | Substituent | Pharmacokinetic Properties | | | | | |
|---|---|---|---|---|---|---|---|
| | | Absorption | | Distribution | | Metabolism | Excretion |
| | | Caco2 permeability | Intestinal absorption (human) | VDss (human) | BBB permeability | CYP2D6 inhibitor | Renal OCT2 substrate |
| 54 | 3-NO2, 4-Cl | 0.081 | 86.147 | -1.111 | -1.168 | No | No |
| 55 | 3,4,5-F | 1.073 | 95.127 | -1.244 | -1.074 | No | No |
| 56 | 2-Cl, 4-NO2 | 0.081 | 86.147 | -1.111 | -1.168 | No | No |
| 57 | 2,4,6-Cl | 1.028 | 92.420 | -0.856 | -0.976 | No | No |
| 58 | 3,4-OCH3 | 1.113 | 97.396 | -1.024 | -0.928 | No | No |
| 59 | 3,4,5-OCH3 | 0.248 | 83.049 | -1.161 | -1.157 | No | No |
| 60 | 2,4-NO2 | 0.085 | 81.997 | -1.361 | -1.529 | No | No |
| 61 | 2,4-OCH3 | 1.113 | 97.396 | -1.024 | -0.928 | No | No |
| 62 | 3-NO2, 4-CH3 | 0.193 | 85.439 | -1.041 | -0.993 | No | No |
| 63 | 2-Cl, 4-F | 1.060 | 94.983 | -0.955 | -0.840 | No | No |
| 64 | 3, CH3, 4-F | 1.082 | 96.442 | -0.885 | -0.665 | No | No |
| 65 | 2,3,4,5-F | 1.070 | 94.368 | -1.401 | -1.275 | No | No |
| 66 | 2,3,4,6-F | 1.070 | 94.368 | -1.401 | -1.275 | No | No |
| 67 | 2,6-F, 4-OCH3 | 1.091 | 95.882 | -1.217 | -1.102 | No | No |
| 68 | 3,5-Cl, 4-OCH3 | 1.061 | 94.077 | -0.996 | -1.036 | No | No |
| 69 | 2,4-F,3-Cl | 1.058 | 94.225 | -1.120 | -1.042 | No | No |
| 70 | 3-Cl, 4-F | 1.060 | 94.983 | -0.955 | -0.840 | No | No |
| 71 | 3-F, 4-OCH3 | 1.094 | 96.641 | -1.053 | -0.901 | No | No |
| 72 | 3-F, 4-CH3 | 1.082 | 96.442 | -0.885 | -0.665 | No | No |
| 73 | 2-F, 4-Br | 1.056 | 94.916 | -0.943 | -0.849 | No | No |
| 74 | 3-CH3, 4-Br | 1.063 | 95.472 | -0.742 | -0.641 | No | No |
| 75 | 2,5-F, 4-Cl | 1.058 | 94.225 | -1.120 | -1.042 | No | No |
| 76 | 3-CF3, 4-F | 1.311 | 97.441 | 0.997 | 0.806 | No | No |
| 77 | 4-sulfonylfluoride | -0.075 | 83.293 | -1.284 | -1.234 | No | No |
| 78 | 4-thiophen | 1.130 | 95.107 | -0.889 | -0.632 | No | No |
| 79 | Naphthoyl | 1.137 | 96.635 | -0.814 | -0.437 | No | No |
| 80 | Lead compound | 1.081 | 97.403 | -0.744 | -0.471 | No | No |

**Table 2.** Toxicity profile.

| No | Substituent | Toxicity | | |
|---|---|---|---|---|
| | | AMES toxicity | Oral Rat Acute Toxicity (LD50) | Hepatotoxicity |
| 1 | 4-phenyldiazen | Mutagen | 2.433 | Yes |
| 2 | 4-chloromethyl | Non-mutagen | 2.720 | Yes |
| 3 | 4-dimethylamino | Non-mutagen | 2.822 | Yes |
| 4 | 2-chloromethyl | Non-mutagen | 2.745 | Yes |
| 5 | 3-CF3 | Non-mutagen | 2.887 | Yes |
| 6 | 3-phenyl acetate | Non-mutagen | 2.801 | Yes |
| 7 | 4-methylthio | Non-mutagen | 2.864 | Yes |
| 8 | 2-CF3 | Non-mutagen | 3.079 | Yes |
| 9 | 3-OCF3 | Non-mutagen | 3.032 | Yes |
| 10 | 4-trifluoromethylthio | Non-mutagen | 3.203 | Yes |
| 11 | 4-trifluoromethoxy | Non-mutagen | 3.032 | Yes |
| 12 | 4-sulfonylchloride | Mutagen | 2.705 | Yes |
| 13 | 4-difluoromethylthio | Non-mutagen | 3.139 | Yes |
| 14 | 4-difluoromethoxy | Mutagen | 2.951 | Yes |
| 15 | 3,5-CF3 | Non-mutagen | 3.259 | Yes |
| 16 | 2-F, 5-CF3 | Non-mutagen | 2.089 | No |
| 17 | 2,5-CF3 | Non-mutagen | 3.259 | Yes |
| 18 | 2-CF3, 4-F | Non-mutagen | 3.082 | Yes |
| 19 | 2-F, 4-CF3 | Non-mutagen | 3.082 | Yes |
| 20 | 3-F, 4-CF3 | Non-mutagen | 3.082 | Yes |
| 21 | 2-F, 3-CF3 | Non-mutagen | 3.082 | Yes |
| 22 | 2-CF3, 5-F | Non-mutagen | 3.082 | Yes |
| 23 | 2,4-CF3 | Non-mutagen | 3.259 | Yes |

| No | Substituent | Toxicity | | |
|---|---|---|---|---|
| | | AMES toxicity | Oral Rat Acute Toxicity (LD50) | Hepatotoxicity |
| 24 | 2,6-CF3 | Non-mutagen | 3.259 | Yes |
| 25 | 2-Cl, 4-CF3 | Non-mutagen | 3.184 | Yes |
| 26 | 3,5-Cl 4-OCH3 | Non-mutagen | 2.987 | No |
| 27 | 2-F, 3-Cl, 5-CF3 | Non-mutagen | 3.172 | Yes |
| 28 | 2-F, 3-Cl, 6-CF3 | Non-mutagen | 3.172 | Yes |
| 29 | 3-F, 5-CF3 | Non-mutagen | 2.089 | No |
| 30 | 3-Cl, 6-CF3 | Non-mutagen | 3.184 | Yes |
| 31 | 4-thiadiazol | Mutagen | 2.822 | Yes |
| 32 | 3-CF3, 4-CH3 | Non-mutagen | 3.097 | Yes |
| 33 | 4-pyrazol | Mutagen | 2.819 | Yes |
| 34 | 4-bromomethyl | Mutagen | 2.359 | Yes |
| 35 | 2,3,4,5,6-F | Non-mutagen | 2.837 | Yes |
| 36 | 2-phenylbenzoate | Non-mutagen | 2.949 | Yes |
| 37 | 4-ethyl | Non-mutagen | 2.819 | Yes |
| 38 | 2-CN | Non-mutagen | 2.811 | Yes |
| 39 | 3-CN | Non-mutagen | 2.811 | Yes |
| 40 | 4-CN | Non-mutagen | 2.811 | Yes |
| 41 | 4-propyl | Non-mutagen | 2.800 | Yes |
| 42 | 4-I | Non-mutagen | 2.785 | No |
| 43 | 4-butyl | Non-mutagen | 2.775 | Yes |
| 44 | 4-heptyl | Non-mutagen | 2.767 | Yes |
| 45 | 4-hexyl | Non-mutagen | 2.768 | Yes |
| 46 | 4-octyl | Non-mutagen | 2.712 | Yes |
| 47 | 4-decyl | Non-mutagen | 2.662 | Yes |
| 48 | 4-butoxy | Non-mutagen | 2.752 | Yes |
| 49 | 2,4-CH3 | Mutagen | 2.763 | Yes |
| 50 | 2,4-F | Mutagen | 2.775 | Yes |
| 51 | 3,4-F | Mutagen | 2.775 | Yes |
| 52 | 2,4,6-CH3 | Non-mutagen | 2.792 | Yes |
| 53 | 2,4,5-F | Mutagen | 2.803 | Yes |
| 54 | 3-NO2, 4-Cl | Mutagen | 2.463 | No |
| 55 | 3,4,5-F | Mutagen | 2.803 | Yes |
| 56 | 2-Cl, 4-NO2 | Mutagen | 2.463 | No |
| 57 | 2,4,6-Cl | Non-mutagen | 3.153 | No |
| 58 | 3,4-OCH3 | Mutagen | 2.650 | Yes |
| 59 | 3,4,5-OCH3 | Mutagen | 2.603 | Yes |
| 60 | 2,4-NO2 | Mutagen | 2.289 | Yes |
| 61 | 2,4-OCH3 | Mutagen | 2.650 | Yes |
| 62 | 3-NO2, 4-CH3 | Mutagen | 2.394 | Yes |
| 63 | 2-Cl, 4-F | Mutagen | 2.907 | Yes |
| 64 | 3, CH3, 4-F | Mutagen | 2.772 | Yes |
| 65 | 2,3,4,5-F | Mutagen | 1.824 | Yes |
| 66 | 2,3,4,6-F | Mutagen | 1.824 | Yes |
| 67 | 2,6-F, 4-OCH3 | Mutagen | 2.744 | Yes |
| 68 | 3,5-Cl, 4-OCH3 | Non-mutagen | 2.987 | No |
| 69 | 2,4-F,3-Cl | Non-mutagen | 2.927 | Yes |
| 70 | 3-Cl, 4-F | Mutagen | 2.907 | Yes |
| 71 | 3-F, 4-OCH3 | Mutagen | 2.716 | Yes |
| 72 | 3-F, 4-CH3 | Mutagen | 2.772 | Yes |
| 73 | 2-F, 4-Br | Mutagen | 2.908 | Yes |
| 74 | 3-CH3, 4-Br | Non-mutagen | 2.906 | Yes |
| 75 | 2,5-F, 4-Cl | Non-mutagen | 2.927 | Yes |
| 76 | 3-CF3, 4-F | Non-mutagen | 2.089 | No |
| 77 | 4-sulfonylfluoride | Mutagen | 2.684 | Yes |
| 78 | 4-thiophen | Non-mutagen | 2.869 | Yes |
| 79 | Naphthoyl | Mutagen | 2.761 | Yes |
| 80 | Lead compound | Mutagen | 1.701 | Yes |

above the threshold of 0.9 log Papp and human intestinal absorption rates above 90%, indicating that compounds with moderate lipophilic substituents such as short alkyl groups and trifluoromethyl ($CF_3$) groups have the potential for good oral bioavailability. Conversely, compounds with large polar substituents such as $NO_2$ and $SO_2Cl$ show reduced absorption capacity, with values < 82%, making them less ideal for further development. In terms of distribution, the volume of distribution (VDss) values are mostly negative (approximately –0.3 to –1.5 log L/kg), indicating a tendency for the compound to remain in plasma rather than in tissues.

Interestingly, long aliphatic substituents (e.g., 4-heptyl, 4-octyl, and 4-decyl) produced VDss values close to neutral, indicating increased distribution to tissues. For blood–brain barrier (BBB) penetration, most compounds show negative values (< –0.5 log BB) and are therefore unlikely to penetrate the brain, except for some $CF_3$ and fluorine derivatives (e.g., 2,5-F-5-$CF_3$ and 3-$CF_3$, 4-F) that have positive values close to 0.8, making them potentially capable of targeting the central nervous system. From a metabolic perspective, all compounds are predicted not to inhibit the CYP2D6 enzyme, which is an important advantage as it reduces the risk of drug interactions. Furthermore, none of the compounds are substrates for the renal transporter OCT2, suggesting that elimination is likely to depend more on hepatic metabolism than renal excretion. Overall, this analysis confirms that compounds with trifluoromethyl substituents and fluorine derivatives are more promising due to their combination of high absorption, better distribution, and BBB penetration for brain targeting, while compounds with large polar substituents should be eliminated from drug design priorities.

The toxicity prediction results (Table 2) indicate that the lead compound has an unfavorable profile because it is identified as mutagenic (positive AMES test) and hepatotoxic and has a relatively low oral rat $LD_{50}$ value (1.701 mol/kg), which indicates a higher level of acute toxicity than most of its derivatives.

Certain groups such as azo, nitro, sulfonyl, and heterocyclic (pyrazole and thiadiazole) are strongly associated with mutagenic properties. These findings are consistent with the literature, in which azo and nitro groups are often identified as structural alerts that can potentially cause mutagenesis through the formation of reactive metabolites (Mortelmans and Zeiger 2000; Kazius et al. 2005). Conversely, most trifluoromethyl (–$CF_3$, –$OCF_3$) and long-chain alkyl (butyl to decyl) substituents were identified as non-mutagenic, with higher $LD_{50}$ values (>3.0 mol/kg), making them relatively safer in terms of acute toxicity. This is consistent with reports that the addition of fluorine groups and lipophilic substituents can increase metabolic stability and reduce the risk of toxic bioactivation (Purser et al. 2008).

However, predictions of hepatotoxicity remain a concern because most compounds, including non-mutagenic derivatives, still show potential liver toxicity. Some substituents such as 2-F,5-$CF_3$; 3,5-Cl,4-$OCH_3$; and 2,4,6-Cl are predicted to be non-hepatotoxic, suggesting that steric factors and electron-withdrawing properties may contribute to reducing the formation of hepatotoxic metabolites (Guengerich 2011). Therefore, these results imply that compound design optimization strategies should avoid high-risk groups (nitro, sulfonyl, and aromatic heterocycles) and instead utilize $CF_3$, $OCF_3$, or lipophilic alkyl substituents to obtain candidates with better safety profiles. Overall, these pkCSM prediction data can serve as a starting point for redesigning lead compounds using a structure–toxicity relationship approach before proceeding to *in vitro* and *in vivo* experimental validation.

## Receptor analysis

In structure-based computational studies, receptor quality validation is an important step before further analyses such as molecular docking or molecular dynamics. One widely used platform is the SAVES server (Structural Analysis and Verification Server), which integrates various methods for assessing protein structure quality, including Ramachandran plot analysis to evaluate the distribution of φ-ψ torsion angles of residues and ERRAT analysis to examine non-bonded atom interaction patterns. This evaluation aims to ensure that protein structures obtained from databases such as the Protein Data Bank (PDB) have adequate geometry and stereochemical quality so that the results of computational simulations can be interpreted accurately and reliably (Ramachandran et al. 1963; Colovos and Yeates 1993).

### *a. Receptor PI3K (3L54.pdb)*

The PI3K receptor (PDB ID: 3L54) is one of the important molecular targets in cellular signaling pathways that play a role in regulating cell proliferation, differentiation, and survival. Before being used in further computational studies, the structure of this protein needs to be validated through quality testing using the SAVES server to ensure the reliability of its crystallographic data. Analysis using the Ramachandran plot and ERRAT provides an overview of the stereochemical quality and patterns of non-bonded atom interactions, thereby assessing the suitability of this model for use in *in silico* simulations such as molecular docking and molecular dynamics (Ramachandran et al. 1963; Colovos and Yeates 1993). The results are shown in Fig. 2.

The results of PI3K structure validation through the SAVES server (Fig. 2) show that 89.5% of residues are in the most favored regions of the Ramachandran plot, 10.1% are in additional allowed regions, and only 0.3% of residues (2 residues) fall into disallowed regions. Although slightly below the ideal standard of greater than 90%, this value still indicates good and acceptable geometric quality for computational studies, as the number of outlier residues is very small and likely located in flexible loop regions (Ramachandran et al. 1963). ERRAT2 analysis provides an overall quality factor of 94.9%, which is well above the 90% threshold and indicates global structural reliability (Colovos and Yeates 1993). Thus, the

PI3K structure is of fairly high quality and is suitable for advanced *in silico* analyses such as molecular docking and molecular dynamics.

### *b. Receptor mTOR (4JT6.pdb)*

The mTOR receptor (PDB ID: 4JT6) is a key protein in the PI3K/Akt/mTOR pathway that regulates cell growth, metabolism, and survival and is an important target in cancer therapy. Before being used in computational studies, the structure of this protein was validated using the SAVES server to assess the quality of its geometry and atomic interactions. The results are shown in Fig. 3.

The results of mTOR protein structure validation using the SAVES server show that 84.5% of residues are in the most favored regions of the Ramachandran plot, 13.1% are in additional allowed regions, 1.5% are in generously allowed regions, and 0.9% of residues (23 residues) are identified in disallowed regions. This value is below the ideal quality standard (greater than 90% in the most favored regions), indicating some conformational instability, especially in loop or flexible domain areas (Ramachandran et al. 1963). ERRAT2 analysis supports these findings with an overall quality factor of 84.1%, which is lower than the high-quality standard (>90%) but still within the acceptable range for preliminary *in silico* analysis (Colovos and Yeates 1993). The presence of several high-error peaks on the ERRAT graph indicates potential local problems in non-bonded atom geometry, particularly in the residue segments around 1440, 1580, and 1620.

Overall, although this mTOR structure is not as robust as models with high Ramachandran and ERRAT scores, it can still be used in advanced computational studies such as molecular docking and molecular dynamics, provided that refinement or energy minimization procedures are carried out to correct residues in disallowed regions. Thus, this structure is suitable for use, but the results of the study should be interpreted with caution, especially in domains that show quality anomalies.

## Molecular docking

In molecular docking analysis using AutoDock, several key parameters are used to ensure the accuracy of ligand–receptor interaction predictions. The initial stage involves determining the grid box, which defines the ligand search area at the active site of the protein. For the PI3K receptor (PDB ID: 3L54), the grid box was set to 30 × 40 × 40, with the grid center at coordinates (24.803, 15.683, 21.651) based on the position of the natural LXX ligand. Meanwhile, the mTOR receptor (PDB ID: 4JT6) used a grid box measuring 40 × 40 × 40, with the grid center at coordinates (52.149, –0.071, –47.665), referring to the natural ligand X6K. Determining this grid is important to ensure that the docking process focuses on the relevant binding site.

Next, the docking results were analyzed based on root mean square deviation (RMSD), free energy of binding (FEB), and inhibition constant (Ki). The RMSD value reflects the stability of the docked ligand position relative to the reference ligand, FEB indicates the strength of the ligand–receptor interaction, and Ki provides an estimate of ligand inhibitory potential. In the docking results, the natural ligand on the PI3K receptor had an RMSD value of 1.266 Å, an FEB of –8.09 kcal/mol, and a Ki of 1.17 μM. In contrast, for the mTOR receptor, the RMSD was 0.389

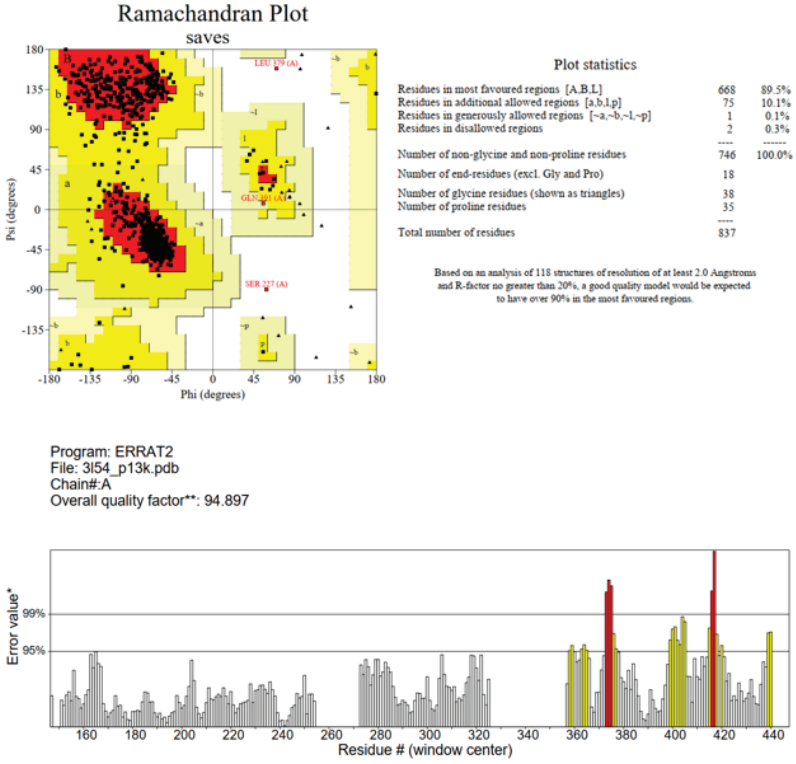


**Figure 2.** Ramachandran plot and ERRAT test results of the PI3K receptor.

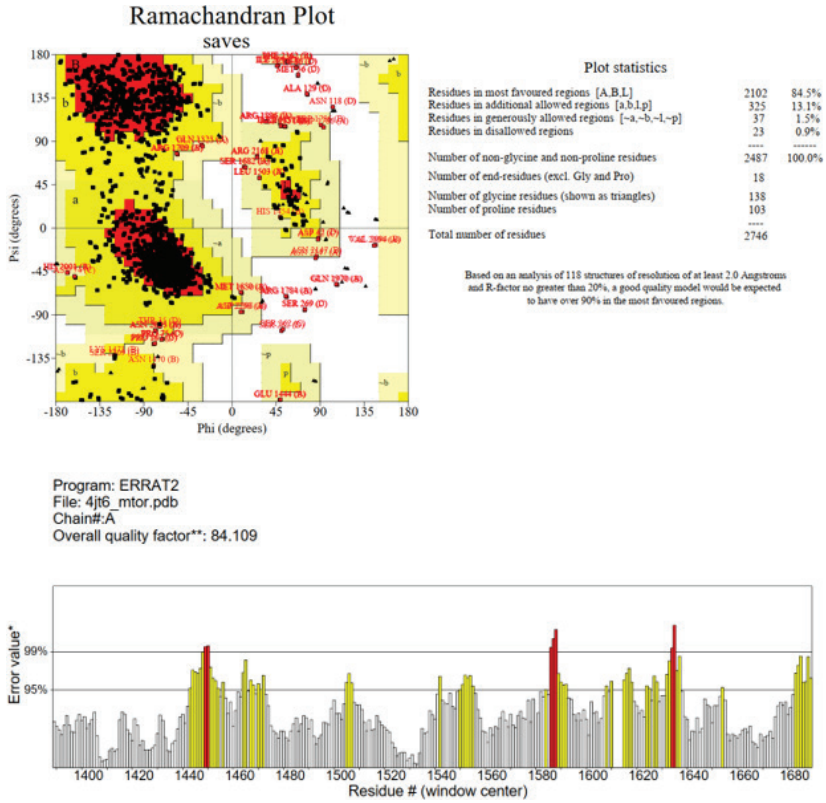


**Figure 3.** Ramachandran plot and ERRAT test results of the mTOR receptor.

Å, the FEB was –9.67 kcal/mol, and the Ki was 0.081 μM. These data indicate that the natural mTOR ligand binds more stably and has a higher affinity than the natural PI3K ligand and can therefore be used as a reference for evaluating the performance of hybrid compounds developed as dual PI3K/mTOR inhibitors (Morris et al. 2009; Trott and Olson 2010). The docking results for the PI3K receptor are shown in Table 3, and those for the mTOR receptor are shown in Table 4. The two-dimensional visualization of compound 78 (4-thiophen) with PI3K and mTOR is shown in Fig. 4**.**

The results of hybrid compound docking against the PI3K receptor (3L54), as shown in Table 3, indicate that several derivatives have stronger binding affinities than natural ligands. The 2-phenylbenzoate compound ranks highest, with a free energy of binding (FEB) value of –9.49 kcal/mol and an inhibition constant (Ki) of 0.111 μM, with hydrogen bond interactions at Val882 and Lys833, as well as hydrophobic bond support with key residues such as Met953, Ile963, Ile881, Asp964, and Tyr867.

The 4-thiadiazole and 2,4-$NO_2$ compounds also showed high affinity (FEB of –9.16 and –9.14 kcal/mol, respectively; Ki 0.192–0.198 μM), with interaction patterns involving the active residues Asp964, Val882, Tyr867, and Lys890, consistent with the binding pocket of natural ligands.

For comparison, the natural ligand on PI3K showed an FEB value of –8.09 kcal/mol with a Ki of 1.17 μM, interacting with residues Tyr867, Asp841, Asp964, Phe965, Lys833, Met953, Ile963, Ile879, Ile831, and Val882. This confirms that some hybrid compounds, especially 2-phenylbenzoate, have stronger bonds (ΔFEB ~ –1.4 kcal/mol lower) and greater inhibitory potential than natural ligands. Overall, these results indicate that structural modifications in hybrid compounds can enhance interactions with key residues in the PI3K active site, making them promising candidates for PI3K inhibitors in cancer therapy.

The docking results of hybrid compounds against the mTOR receptor (4JT6), as shown in Table 4, indicate that several derivatives are able to exceed the performance of natural ligands in terms of binding affinity. The 4-phenyldiazen and 2-CN compounds have the highest free energy of binding (FEB) values, respectively, of –10.07 kcal/mol, with an inhibition constant (Ki) of approximately 0.041 μM, which is better than the natural ligand, with an FEB of –9.67 kcal/mol and a Ki of 0.081 μM. Both show hydrogen bonding interactions with important residues in the mTOR binding site, including Asp2357, Cys2243, Val2240, Trp2239, Ile2237, and Tyr2225, and are reinforced by hydrophobic interactions with Met2345, Ile2356, and Leu2185.

In addition, the compounds 3,4,5-$OCH_3$ (–9.95 kcal/mol; Ki 0.099 μM) and 4-thiophen (–9.88 kcal/mol; Ki 0.057 μM) also showed consistent interactions with active residues, indicating their potential as potent inhibitors. This pattern confirms that aromatic substituents with electron-withdrawing groups and heteroaromatics can increase the affinity of ligands for mTOR.

In comparison, natural ligands interact with residues Val2240, Tyr2225, Asp2195, Met2345, Ile2237, Ile2356, and Trp2239, with lower binding affinities than the leading hybrid compound. This shows that the design of certain hybrid compounds is not only capable of maintaining key

**Table 3.** Docking results of the design hybrid compound against the PI3K receptor.

| NO | Substituen | FEB (kcal/mol) | KI (μM) | RUN | INTERACTION | |
|---|---|---|---|---|---|---|
| | | | | | HYDROGEN BOND | HYDROPHOBIC BOND |
| 36 | 2-phenylbenzoate | -9.49 | 0.1113 | 92 | Val882, Lys833 | Met953, Ile881, Ala885, Ile963, Asp964, Ile879, Lys833, Met804, Pro810, Tyr867 |
| 31 | 4-thiadiazol | -9.16 | 0.1929 | 24 | Phe965, Asp964, Val882 | Ile831, Ile879, Tyr867, Ile963, Val882, Phe961, Ala885, Met953, Ile881, Cys869, Asp964 |
| 60 | 2,4-NO2 | -9.14 | 0.19854 | 65 | Thr887, Lys890, Tyr867, Asp964 | Met953, Phe961, Ile963, Ile831, Tyr867, Val882, Asp964 |
| 78 | 4-thiophen | -9.03 | 0.23906 | 83 | Val882 | Ala885, Met953, Ile881, Trp812, Asp964, Ile831, Asp841, Lys833, Ile879, Ile963, Tyr867, Val882 |
| 12 | 4-sulfonylchloride | -8.95 | 0.27455 | 62 | Lys833, | Ile831, Ile963, Met953, Ala885, Tyr867, Ile881, Ile879, Asp964, Trp812, Val882 |
| 56 | 2-Cl, 4-NO2 | -8.94 | 0.27953 | 94 | Ala805, Lys890, Tyr867, Asp964 | Met804, Lys833, Ile963, Ile879, Asp964 |
| 62 | 3-NO2, 4-CH3 | -8.94 | 0.28189 | 29 | Lys890, Thr887, Thr867, Asp964 | Met953, Met804, Trp812, Ile963, Ile879, Asp964 |
| 54 | 3-NO2, 4-Cl | -8.91 | 0.29403 | 37 | Thr887, Lys890, Tyr867, Asp964 | Met953, Trp812, Ile879, Ile963, Asp964 |
| 59 | 3,4,5-OCH3 | -8.88 | 0.31026 | 62 | Val882, Tyr867, Lys833, Asp836, Asp841 | Ile963, Ile879, Met953, Val882, Ile881, Ala885, Tyr867, Asp964 |
| 33 | 4-pyrazol | -8.8 | 0.35208 | 53 | Val882, Asp836 | Trp812, Ile881, Ala885, Met953, Val882, Tyr867, Ile963, Ile879, Lys833, Ile831, Asp964 |
| 79 | naftoyl | -8.79 | 0.35976 | 39 | Asp836, Lys833, Asp964, Val882 | Asp964, Met953, Ile963, Phe961, Tyr867, Ile831, Ile879 |
| 6 | 3-phenyl acetat | -8.67 | 0.44417 | 2 | Val882, Lys833 | Asp841, Ile879, Ile963, Met953, Ala885, Ile881, Tyr867, Lys833, Asp964 |
| 74 | 3-CH3, 4-Br | -8.66 | 0.44854 | 14 | Val882 | Tyr867, Met953, Ile963, Ile831, Ile879, Lys833, Asp964, Ile881, Ala885 |
| 42 | 4-I | -8.65 | 0.45599 | 62 | Val882 | Tyr867, Ile963, Asp964, Ile831, Ile879, Met853, Ile881, Ala885, Val882 |
| 44 | 4-heptyl | -8.56 | 0.5317 | 30 | Asp836, Lys833, Tyr867, Asp964 | Asp964, Ile879, Ile831, Tyr867, Ile963, Met953 |
| 77 | 4-sulfonylfluoride | -8.52 | 0.56984 | 73 | Asp836, Lys833, Asp964, Val882 | Ile831, Ile963, Met953, Ile879, Asp964 |
| 45 | 4-hexyl | -8.49 | 0.59341 | 23 | Asp964, Tyr867 | Ile879, Ile831, Asp964, Phe961, Met953, Ile963, Tyr867 |
| 73 | 2-F, 4-Br | -8.49 | 0.59463 | 44 | Val882 | Val882, Tyr867, Ala885, Met853, Ile881, Asp964, Ile879, Ile831, Ile963 |
| 47 | 4-decyl | -8.4 | 0.70024 | 35 | Lys890, Asp964 | Pro810, Lys833, Asp950, Ile831, Ile879, Met953, Lys890, Met804 |
| 23 | 2,4-CF3 | -8.39 | 0.71394 | 46 | Phe965, Val882 | Met953, Ile881, Ala885, Tyr867, Ile963, Ile879, Asp841, Lys833, Asp964, Pro810 |
| 48 | 4-butoxy | -8.38 | 0.71663 | 5 | Val882, Asp964 | Ile963, Ile831, Trp812, Ile881, Met953, Ala885, Val882, Tyr867, Ile879, Asp964 |
| 7 | 4-methylthio | -8.35 | 0.75262 | 4 | Val882 | Ile879, Ile831, Asp964, Ile963, Tyr867, Phe961, Met953, Ala885, Ile881 |
| 40 | 4-CN | -8.33 | 0.78055 | 69 | Val882 | Ile831, Ile879, Asp964, Ile963, Val882, Tyr867, Phe961, Ala885, Ile881, Met953 |
| 11 | 4-trifluoromethoxy | -8.32 | 0.79021 | 68 | Val882, Phe965 | Asp841, Ile879, Asp964, Ile963, Met953, Tyr867, Phe961, Ala885, ILe881, Ile831 |
| 43 | 4-butyl | -8.32 | 0.7941 | 51 | Val882 | Tyr867, Met953, Val882, Lys833, Ser806 |
| 61 | 2,4-OCH3 | -8.32 | 0.79372 | 2 | Asp841, Val882 | Ile831, Asp964, Ile963, Ile879, Val882, Tyr867, Met953, Ala885, Ile881 |
| 46 | 4-octyl | -8.3 | 0.82086 | 34 | | Asn951, Asp964, Tyr867, Ile831, Trp812, Met804, Met953, Ile879, Ile963 |
| 34 | 4-bromomethyl | -8.29 | 0.8414 | 3 | Val882 | Ala885, Ile881, Ile879, Ile831, Asp964, Ile963, Tyr867, Met953, Val882 |
| 38 | 2-CN | -8.29 | 0.83879 | 3 | Phe965, Tyr867 | Tyr867, Ile881, Ile963, Val882, Phe961, Met953, Asp964, Ile879, Lys833 |
| 41 | 4-propyl | -8.2 | 0.97032 | 89 | Val882 | Tyr867, Met953, Ile963, Asp964, Ile831, Cys869, Ile879, Leu838, Ile881, Trp812, Ala885 |

| NO | Substituen | FEB (kcal/mol) | KI (μM) | RUN | INTERACTION | |
|---|---|---|---|---|---|---|
| | | | | | HYDROGEN BOND | HYDROPHOBIC BOND |
| 75 | 2,5-F, 4-Cl | -8.2 | 0.96821 | 53 | Val882 | Val882, Tyr867, Ile963, Ile831, Ile879, Asp964, Ile881, Met953, Ala885 |
| 68 | 3,5-Cl, 4-OCH3 | -8.19 | 0.99075 | 35 | Asp836, Lys833, Asp964, Val882 | Ile831, Trp812, Tyr867, Met953, Ile963, Ile879 |
| 71 | 3-F, 4-OCH3 | -8.18 | 1 | 82 | Val882, Asp841 | Tyr867, Val882, Met953, Ile963, Ile879, Ile831, Asp964, Ile881, Ala885 |
| 37 | 4-etyl | -8.17 | 1.02 | 1 | Val882 | Tyr867, Phe961, Ala885, Ile881, Met953, Asp964, Ile831, Ile879, Ile963, Val882 |
| 49 | 2,4-CH3 | -8.16 | 1.04 | 1 | Asp964, Tyr867 | Lys833, Ile879, Pro810, Ile881, Met953, Ala885, Trp812, Phe961, Tyr867, Asp964, Met804, Ile831 |
| 26 | 3,5-Cl 4-OCH3 | -8.14 | 1.08 | 23 | ASp836, Lys833, Asp964 | Asp964, Ile831, Ile963, Met953, Tyr867, Trp812, Ile879 |
| 58 | 3,4-OCH3 | -8.11 | 1.14 | 96 | Val882, Asp836, Asp841, Tyr867 | Val882, Ile963, Ile879, Asp964, Tyr867, Ile881, Met953, Ala885 |
| 2 | 4-chloromethyl | -8.08 | 1.21 | 97 | Val882 | Ile831, Ile879, Asp964, Ile963, Tyr867, Ala885, Met953, Ile881 |
| 9 | 3-OCF3 | -8.06 | 1.24 | 31 | Phe965 | Asp841, Ile963, Ile879, Ile881, Val882, Ala885, Met953, Tyr867, Ile831, Asp964, Asp841 |
| 30 | 3-Cl, 6-CF3 | -8.05 | 1.25 | 10 | Val882 | Met953, Ala885, Ile881, Tyr867, Ile963, Ile831, Ile879, Asp964, Met804, Pro810 |
| 39 | 3-CN | -8.01 | 1.34 | 57 | Val882, Lys833 | Asp964, Ile879, Ile963, Val882, Tyr867, Ala882, Met953, Ile881, Ile831 |
| 52 | 2,4,6-CH3 | -8.01 | 1.35 | 38 | Glu880, Asp964 | Ile963, Met804, Pro810, Ile831, Asp964, Ile879, Tyr867, Met953, Ala885, Ile881, Trp812, Phe961 |
| 80 | Lead compound | -8 | 1.36 | 56 | Met953, Val882, Glu880 | Asp964, Ile879, Met953, Trp812, Ile881, Ala885 |
| 4 | 2-chloromethyl | -7.98 | 1.41 | 39 | Asp964 | Ile879, Ala885, Ile881, Val882, Met953, Phe961, Ile963, Tyr867, Lys833, Asp964 |
| 10 | 4-trifluoromethylthio | -7.96 | 1.47 | 41 | Asp964, Phe965, Val882 | Asp841, Ile9879, Ile831, Ile963, Met953, Tyr867, Ala885, Ile881, Asp964 |
| 14 | 4-difluoromethoxy | -7.93 | 1.53 | 19 | Val882, Phe965 | Asp841, Ile963, Tyr867, Met953, Ala885, Ile881, Ile879, Asp964, Ile831 |
| 3 | 4-dimethylamino | -7.91 | 1.61 | 73 | Lys833, Asp964, Val882, Glu880, Asp836 | Ile963, Met953, Ile879, Asp964, Ile831 |
| 8 | 2-CF3 | -7.89 | 1.54 | 5 | Val882 | Met953, Ala885, Ile881, Tyr867, Ile879, Ile963, Ile831, Asp964, Met804 |
| 69 | 2,4-F,3-Cl | -7.81 | 1.87 | 5 | Asp964, Val882 | Tyr867, Val882, Met953, Ile963, Ile831, Asp964, Ile879, Lys833, Ile881, Ala885 |
| 63 | 2-Cl, 4-F | -7.75 | 2.1 | 14 | Val882 | Tyr867, Ala885, Ile881, Ile879, Lys833, Ile831, Pro810, Asp964, Ile963, Met953, Val882 |
| 13 | 4-difluoromethylthio | -7.74 | 2.11 | 76 | Ser806, Lys833, Tyr867 | Ile879, Ile963, Asp964, Met804, Pro810, Ala805 |
| 72 | 3-F, 4-CH3 | -7.73 | 2.16 | 50 | Val882 | Met953, Tyr867, Ile963, Asp964, Ile831, Ile879, Ile881, Ala885, Val882 |
| 24 | 2,6-CF3 | -7.7 | 2.28 | 99 | Asp964 | Lys833, Ile879, Ile963, Glu880, Phe961, Tyr867, Val882, Met953, Ala885, Trp812, Asp964 |
| 70 | 3-Cl, 4-F | -7.7 | 2.27 | 68 | Val882, Asp964 | Tyr867, Val882, Met953, Ile963, Ile831, Asp964, Lys833, Ile879, Ile881, Ala885 |
| 76 | 3-CF3, 4-F | -7.7 | 2.26 | 51 | Lys833, Val882 | Ile831, Ile879, Asp964, Ile963, Ile881, Met953, Val882, Ala885, Tyr867 |
| 18 | 2-CF3, 4-F | -7.69 | 2.32 | 33 | Asp964, Tyr867, Ser806 | Asp964, Ile963, Tyr867, Ala885, Val882, Met953, Ile881, Pro810 |
| 64 | 3, CH3, 4-F | -7.69 | 2.3 | 21 | Val882 | Tyr867, Val882, Met853, Ile963, Asp964, Ile831, Lys833, Ile879, Ile881, Phe961, Ala885 |
| 29 | 3-F, 5-CF3 | -7.67 | 2.39 | 40 | Lys833, Val882 | Ile963, Met953, Val882, Tyr867, Ala885, Ile881, Ile831, Ile879, Asp964, Lys833 |
| 16 | 2-F, 5-CF3 | -7.65 | 2.48 | 11 | Lys833, Val882 | Ile963, Met953, Tyr867, Ala885, Ile881, Asp964, Ile831, Ile879 Lys833 |
| 5 | 3-CF3 | -7.64 | 2.53 | 36 | Lys833, Val882 | Asp964, Ile879, Ile831, Ile963, Met953, Ile881, Ala885, Tyr867 |
| 17 | 2,5-CF3 | -7.63 | 2.54 | 13 | Tyr867, Met953, Val882, Lys833, Ser806 | Ile963, Asp964, Tyr867, Met953, Val882, Ala885, Ile881, Lys833, Pro810, Met804 |

| NO | Substituen | FEB (kcal/mol) | KI (μM) | RUN | INTERACTION | |
|---|---|---|---|---|---|---|
| | | | | | HYDROGEN BOND | HYDROPHOBIC BOND |
| 35 | 2,3,4,5,6-F | -7.63 | 2.54 | 43 | Lys833, Asp964, Tyr867 | Ile879, Ile831, Met953, Ile881, Ala885, Trp812, Phe961, Tyr867, Asp964, Met804 |
| 22 | 2-CF3, 5-F | -7.62 | 2.59 | 55 | Val882 | Tyr867, Ile963, Asp841, Ile879, Asp964, Ile831, Met953, Ala885, Ile881, Val882 |
| 21 | 2-F, 3-CF3 | -7.61 | 2.65 | 87 | Lys833, Val882 | Asp964, Ile9879, Ile963, Val882, Tyr867, Ile881, Met953, Ala885, Lys833 |
| 32 | 3-CF3, 4-CH3 | -7.6 | 2.68 | 7 | Asp836, Lys833, Asp964 | Tyr867, Ile963, Met953, Ile879, Asp964, Ile831, Glu880 |
| 50 | 2,4-F | -7.54 | 2.97 | 67 | Val882, Asp964 | Ile831, Ile879, Ile963, Tyr867, Ala885, Met953, Ile881, Asp964 |
| 65 | 2,3,4,5-F | -7.54 | 2.95 | 5 | Val882 | Tyr867, Val882, Met953, Ile963, Ile831, Asp964, Ile879, Ile881, Ala885 |
| 55 | 3,4,5-F | -7.51 | 3.14 | 83 | Val882 | Tyr867, Val882, Met953, Ile963, Asp964, Ile831, Ile879, Ile881, Phe961, Ala885 |
| 51 | 3,4-F | -7.5 | 3.16 | 31 | Val882 | Met953, Ile963, Ile879, Asp964, Ile831, Ile881, Ala885, Tyr867 |
| 66 | 2,3,4,6-F | -7.5 | 3.19 | 62 | Tyr867, Asp964 | Ile881, Met953, Trp812, Phe961, Val882, Ala885, Tyr867, Asp964, Ile831, Ile879 |
| 1 | 4-phenyldiazen | -7.48 | 3.31 | 93 | Lys807, Val882 | Met953, Ala885, Ile881, Tyr867, Ile879, Ile963, Trp812, Asp964, Met804 |
| 20 | 3-F, 4-CF3 | -7.48 | 3.29 | 34 | Val882, ASp964 | Ile879, Ile831, Ile963, Tyr867, Val882, Ala885, Met953, Ile881, Asp964, Asp841 |
| 27 | 2-F, 3-Cl, 5-CF3 | -7.48 | 3.27 | 61 | Lys833, Tyr867 | Asp964, Ile831, Met853, Glu880, Ile963, Trp812, Ile879 |
| 53 | 2,4,5-F | -7.46 | 3.42 | 46 | Val882 | Tyr867, Ala885, Met953, Ile881, Asp964, Ile963, Ile879, Ile831 |
| 57 | 2,4,6-Cl | -7.45 | 3.48 | 23 | Tyr867 | Lys833, Asp964, Ile831, Trp812, Val882, Ile963, Met953, Ile879 |
| 15 | 3,5-CF3 | -7.38 | 3.9 | 43 | Phe965, Asp964, Tyr867 | Asp841, Ile879, Ile963, Met953, Met804, Trp812, Pro810, Ile881, Phe961, Lys833, Ile831, Asp964 |
| 67 | 2,6-F, 4-OCH3 | -7.37 | 3.94 | 76 | Asp836, Glu880 | Ile879, Tyr867, Asp964, Ile963, Met953, Ile831 |
| 25 | 2-Cl, 4-CF3 | -7.27 | 4.69 | 56 | Asp964 | Asp841, Asp964, Ile879, Ile963, Tyr867, Val882, Ala885, Met953, Ile881, Lys833, Pro810, Ile831 |
| 28 | 2-F, 3-Cl, 6-CF3 | -7.19 | 5.4 | 61 | Trp867, Asp964, Val882 | Lys833, Pro810, Ile831, Met804, Asp964, Tyr867, Glu880, Ile881, Ala885, Phe961, Met953, Val882, Trp812 |
| 19 | 2-F, 4-CF3 | -7.17 | 5.56 | 51 | Asp964, Val882 | Asp841, Ile831, Ile879, Ile963, Tyr867, Ala885, Met953, Ile881, Asp964 |
| | Native ligand | -8.09 | 1.17 | 3 | Tyr867, Asp841 | Met953, Ile963, Met804, Tyr867, Asp964, Phe965, Lys833, Ile879, Ile831, Val882 |

**Table 4.** Docking results of the hybrid compound design against mTOR receptor.

| NO | Substituen | FEB (kcal/mol) | KI (μM) | RUN | INTERACTION | |
|---|---|---|---|---|---|---|
| | | | | | HYDROGEN BOND | HYDROPHOBIC BOND |
| 1 | 4-phenyldiazen | -10.07 | 0.04145 | 82 | Asp2357, Cys2243, Val2240, Trp2239 | Met2345, Thr2245, Trp2239, Ile2356, Ile2237, Tyr2225, Leu2185, Leu2192 |
| 38 | 2-CN | -10.07 | 0.0418 | 30 | Ile2237, Gly2238, Trp2239, Val2240, Asp2357, Tyr2225, Asp2195, Glu2190 | Ile2237, Ile2356, Cys2243, Trp2239, Met2345 |
| 59 | 3,4,5-OCH3 | -9.95 | 0.09986 | 54 | Val2240, Asp2195, Asp2357 | Asp2195, Ile2356, Ile2237, Tyr2225, Val2240, Met2345, Trp2239, Cys2243 |
| 78 | 4-thiophen | -9.88 | 0.05696 | 40 | Met2345, Cys2243, Val2240, Tyr2225 | Met2345, Trp2239, Gly2238, Ile2356, Leu2185, Ile2237 |
| 12 | 4-sulfonylchloride | -9.87 | 58.26 | 2 | Asp2195, Tyr2225, Ile2237, Val2240, Thr2245 | Ile2356, Trp2239, Met2345, Ile2237 |
| 33 | 4-pyrazol | -9.69 | 0.07886 | 80 | Asp2195, Tyr2225, Ile2237, Val2240 | Ile2356, Ile2237, Met2345, Trp2239, Ala2248 |
| 4 | 2-chloromethyl | -9.44 | 0.12008 | 90 | Val2240, Gly2238, Asp2357 | Ile2237, Val2240, Met2345, Cys2243, Trp2239, Tyr2225, Leu2185, Lys2187, Asp2357 |

| NO | Substituen | FEB (kcal/mol) | KI (μM) | RUN | INTERACTION | |
|---|---|---|---|---|---|---|
| | | | | | HYDROGEN BOND | HYDROPHOBIC BOND |
| 48 | 4-butoxy | -9.19 | 0.18462 | 88 | Val2240, Asp2357 | Ile2237, Ile2356, Trp2239, Cys2243, Met2345, Tyr2225 |
| 39 | 3-CN | -9.11 | 0.20845 | 97 | Asp2195, Tyr2225, Ile2237, Thr2245, Gly2238, Trp2239 | Ile2237, Cys2243, Met2345, Trp2239, Ile2256 |
| 30 | 3-Cl, 6-CF3 | -8.98 | 0.25948 | 62 | Val2240, Lys2187 | Glu2190, Asp2357, Val2227, Ile2237, Tyr2225, Leu2354, Trp2239, Met2345, Cys2243, Val2240 |
| 31 | 4-thiadiazol | -8.98 | 0.2627 | 7 | Tyr2225, Asp2357, Asp2357, Tyr2225 | Val2240, Cys2243, Met2345, Ile2237, Ile2356, Tyr2225, Ile2163, Pro2169, Leu2185, Glu2190, Trp2239 |
| 26 | 3,5-Cl 4-OCH3 | -8.97 | 0.26568 | 34 | Gly2238, Cys2243, Val2240, Tyr2225, Asp2357, Asp2195 | Leu2192, Ile2356, Ile2237, Tyr2225, Val2240, Leu2354, Met2345, Trp2239 |
| 56 | 2-Cl, 4-NO2 | -8.95 | 0.27653 | 13 | Gly2238, Val2240, Asp2195, Asp2357, Tyr2225 | Val2240, Lys2187, Ile2237, Ile2356, Leu2185, Trp2239, Met2345 |
| 68 | 3,5-Cl, 4-OCH3 | -8.92 | 0.28743 | 63 | Glys2238, Tyr2225, Asp2357, Glu2190 | Leu2192, Ile2356, Ile2237, Tyr2225, Val2240, Cys2243, Met2345, Leu2354, Trp2239 |
| 79 | Naphthoyl | -8.92 | 0.29133 | 79 | Val2240, Trp2239 | Trp2239, Met2345, Leu2185, Ile2237, Ile2356 |
| 36 | 2-phenylbenzoate | -8.88 | 0.31009 | 100 | Asp2357 | Ile2237, Ile2356, Val2240, Tyr2225, Cys2243, Trp2239, Met2345 |
| 22 | 2-CF3, 5-F | -8.86 | 0.3196 | 80 | Val2240, Gly2238, Tyr2225, Asp2357 | Asp2195, Ile2237, Leu2192, Ile2356, Met2345, Trp2239, Cys2243, Val2240, Tyr2225 |
| 62 | 3-NO2, 4-CH3 | -8.85 | 0.32786 | 45 | Thr2245, Asp2244, Met2345, Val2240, Trp2239 | Trp2239, Met2345, Leu2185, Ile2237, Ile2356, Tyr2225 |
| 25 | 2-Cl, 4-CF3 | -8.82 | 0.3417 | 12 | Gly2238, Val2240, Tyr2225, Asp2357, Asp2195 | Met2345, Trp2239, Leu2185, Ile2356, Lys2187, Leu2192, Ile2237, Val2240 |
| 60 | 2,4-NO2 | -8.77 | 0.37021 | 71 | Val2240, Cys2243, Met2345, Trp2239 | Ile2237, Leu2185, Ile2356, Trp2239 |
| 46 | 4-octyl | -8.76 | 0.37947 | 86 | Asp2195, Tyr2225, Ile2237, Val2240 | Met2345, Trp2239, Leu2185, Ile2163, Ile2356, Ile2237 |
| 8 | 2-CF3 | -8.74 | 0.39398 | 42 | Glu2190, Asp2195, Asp2357, Tyr2225, Glys2238 | Ile2237, Ile2356, Met2345, Trp2239, Cys2243 |
| 47 | 4-decyl | -8.72 | 0.40773 | 38 | Trp2239, Cys2243 | Met2345, Cys2243, Trp2239, Pro2169, Leu2185, Ile2163 |
| 42 | 4-I | -8.68 | 0.4333 | 90 | Asp2357, Tyr2225, Val2240 | Leu2192, Ile2356, Ile2237, Val2240, Cys2243, Met2345, Trp2239, Leu2354 |
| 74 | 3-CH3, 4-Br | -8.63 | 0.47599 | 54 | Met2345, Val2240, Trp2239 | Ile2356, Ile2237, Leu2185, Trp2239, Met2345 |
| 6 | 3-phenyl acetate | -8.62 | 0.48416 | 87 | Trp2239, Thr2245 | Met2345, Ile2237, Ile2356, Leu2185, Trp2239 |
| 49 | 2,4-CH3 | -8.62 | 0.47961 | 5 | Val2240, Gly2238, Tyr2225, Asp2357 | Ile2237, Lys2187, Ile2356, Pro2169, Leu2185, Val2240, Met2345, Cys2243, Trp2239, Tyr2225 |
| 24 | 2,6-CF3 | -8.6 | 0.50037 | 32 | Ile2237, Val2240, Asp2195 | Ile2356, Leu2185, Val2240, Cys2243, Met2345, Trp2239, Ile2237 |
| 61 | 2,4-OCH3 | -8.56 | 0.53219 | 83 | Thr2245, Gly2238, Glu2190, Asp2195, Val2240, Trp2239 | Met2345, Trp2239, Ile2356, Leu2185, Ile22237 |
| 29 | 3-F, 5-CF3 | -8.52 | 0.56672 | 88 | Val2240 | Cys2243, Met2345, Trp2239, Leu2354, Tyr2225, Ile2237, Leu2192, Asp2195, Glu2190, Asp2357 |
| 41 | 4-propyl | -8.48 | 0.60411 | 88 | Asp2357, Val2240 | Leu2192, Ile2356, Ile2237, Val2240, Leu2354, Met2345, Cys2243, Trp2239 |
| 54 | 3-NO2, 4-Cl | -8.47 | 0.62204 | 61 | Val2240, Met2345, Trp2239 | Met2345, Trp2239, Leu2185, Ile2356, Ile2237 |
| 45 | 4-hexyl | -8.43 | 0.66482 | 9 | | Asp22357, Ile2237, Tyr2225, Ile2356, Leu2185, Trp2239, Met2345, Cys2243 |
| 63 | 2-Cl, 4-F | -8.42 | 0.66812 | 78 | Gly2238, Val2240, Asp2357, Tyr2225, Asp2195 | Lys2187, Ile2356, Ile2237, Leu2185, Trp2239, Met2345 |
| 44 | 4-heptyl | -8.41 | 0.68323 | 44 | Val2240, Cys2243, Trp2239, Met2345 | Leu2237, Leu2185, Ile2356, Ile2163, Trp2239 |
| 77 | 4-sulfonylfluoride | -8.4 | 0.69608 | 16 | Val2240 | Leu2185, Met2345, Ile2356, Tyr2225, Leu2192, Ile2237 |
| 27 | 2-F, 3-Cl, 5-CF3 | -8.39 | 0.7138 | 2 | Glu2190, Asp2195, Gly2238, Thr2245 | Trp2239, Cys2243, Met2345, Ile2256, Ile22237 |
| 34 | 4-bromomethyl | -8.36 | 0.74806 | 83 | Met2345, Val2240, Trp2239 | Trp2239, Leu2185, Ile2237, Ile2356, Met2345 |
| 52 | 2,4,6-CH3 | -8.32 | 0.79375 | 47 | Asp2357, Tyr2225, Val2240, Cys2243, Gly2238 | Met2345, Ile2356, Pro2169, Leu2185, Lys2187, Ile2237, Tyr2225, Trp2239, Cys2243, Gly2238 |

| NO | Substituen | FEB (kcal/mol) | KI (μM) | RUN | INTERACTION | |
|---|---|---|---|---|---|---|
| | | | | | HYDROGEN BOND | HYDROPHOBIC BOND |
| 40 | 4-CN | -8.3 | 0.82879 | 72 | Val2240, Gly2238, Ser2165, Gln2167 | Leu2185, Pro2169, Val2240, Cys2243, Met2345, Tyr2225, Trp2239 |
| 64 | 3, CH3, 4-F | -8.3 | 0.81973 | 19 | Met2345, Val2240, Trp2239 | Met2345, Ile2356, Ile2237, Leu2185, Trp2239 |
| 37 | 4-etyl | -8.29 | 0.84252 | 22 | Met2345, Val2240, Trp2239 | Met2345, Ile2356, Ile2163, Trp2239, Leu2185, Ile2237 |
| 72 | 3-F, 4-CH3 | -8.29 | 0.83548 | 22 | Met2345, Val2240, Trp2239 | Ile2356, Ile2237, Tyr2225, Leu2185, Trp2239, Met2345 |
| 70 | 3-Cl, 4-F | -8.27 | 0.86305 | 90 | Met2345, Val2240, Trp2239 | Trp2239, Met2345, Ile2356, Ile2237, Leu2185, Tyr2225 |
| 43 | 4-butyl | -8.26 | 0.88114 | 55 | Met2345, Val2240, Trp2239 | Ile2163, Ile2356, Ile2237, Leu2185, Trp2239 |
| 58 | 3,4-OCH3 | -8.21 | 0.95825 | 83 | Thr2245, Met2345, Val2240, Cys2243, Gly2238 | Trp2239, Leu2185, Ile2356, Ile2237 |
| 80 | Lead compound | -8.21 | 0.96304 | 58 | Ile2237, Gly2238, Asp2195, Tyr2225, Trp2239 | Met2345, Trp2239, Cys2243, Ile2356, Ile2237 |
| 2 | 4-chloromethyl | -8.19 | 0.99913 | 9 | Met2345, Val2240, Trp2239 | Met2345, Ile2356, Ile2237, Leu2185, Trp2239 |
| 3 | 4-dimethylamino | -8.19 | 0.99288 | 11 | Trp2239, Val2240 | Met2345, Ile2237, Ile2356, Leu2185, Trp2239 |
| 17 | 2,5-CF3 | -8.16 | 1.05 | 18 | Asp2244, Trp2239, Val2240, Ile2237 | Ile2237, Ile2356, Leu2354, Gly2238, Val2240, Met2345, Trp2239, Cys2243 |
| 57 | 2,4,6-Cl | -8.15 | 1.06 | 15 | Val2240, Asp2357, Gly2238 | Cys2243, Met2345, Trp2239, Tyr2225, Ile2356, Pro2169, Ile2163, Leu2185, Lys2187, Ile22237, Val2240 |
| 21 | 2-F, 3-CF3 | -8.14 | 1.07 | 17 | Asp2195, Tyr2225, Ile2237, Gly2238, Thr2245 | Asp2244, Cys2243, Met2345, Trp2239, Ile2356, Ile2237 |
| 76 | 3-CF3, 4-F | -8.13 | 1.11 | 38 | Val2240, Gly2238, Asp2357, Phe2358 | Val2240, Cys2243, Met2345, Trp2239, Tyr2225, Leu2192, Glu2190, Asp2195, Ile2237 |
| 32 | 3-CF3, 4-CH3 | -8.12 | 1.12 | 59 | Tyr2225, Val2240, Gly2238, Lys2187 | Leu2192, Asp2357, Ile2356, Ile2237, Val2240, Leu2354, Met2345, Trp2239, Cys2243, Glu2190 |
| 7 | 4-methylthio | -8.11 | 1.13 | 60 | Met2345, Trp2239, Val2240 | Trp2239, Met2345, Leu2185, Ile2237, Ile2256 |
| 73 | 2-F, 4-Br | -8.11 | 1.13 | 35 | Tyr2225, Gly2238, Val2240, Trp2239 | Ile2237, Met2345, Trp2239, Leu2185, Ile2356 |
| 69 | 2,4-F,3-Cl | -8.1 | 1.15 | 62 | Val2240, Gly2238, Tyr2225, Trp2239 | Leu2185, Met2345, Ile2356, Ile2237, Trp2239 |
| 50 | 2,4-F | -8.07 | 1.21 | 33 | Tyr2225, Ile2237, Cys2243, Trp2239 | Trp2239, Met2345, Cys2243, Val2240, Ile2237, Ile2356, Leu2192 |
| 14 | 4-difluoromethoxy | -8.05 | 1.25 | 14 | Tyr2225, Gly2238, Val2240, Trp2239 | Ile2237, Leu2185, Met2345, Trp2239, Ile2356 |
| 10 | 4-trifluoromethylthio | -8.04 | 1.28 | 71 | Met2345, Thr2245, Trp2239, Val2240 | Ile2356, Ile2237, Leu2185, Trp2239, Met2345 |
| 75 | 2,5-F, 4-Cl | -8.03 | 1.3 | 7 | Met2345, Trp2239, Cys2243 | Val2240, Trp2239, Met2345, Ile2356, Leu2185, Ile2237 |
| 18 | 2-CF3, 4-F | -8.02 | 1.33 | 54 | Cys2243, Ile2237 | Ile2356, Trp2239, Met2345, Val2240, Cys2243, Ile2237 |
| 13 | 4-difluoromethylthio | -7.95 | 1.49 | 41 | Cys2243, Gly2238 | Val2240, Met2345, Trp2239, Leu2192, Asp2195, Ile2356, Ile2237, Cys2243 |
| 67 | 2,6-F, 4-OCH3 | -7.92 | 1.57 | 35 | Val2240, Gly2238, Tyr2225, Asp2357 | Val2240, Met2345, Cys2243, Trp2239, Ile2356, Tyr2225, Ile2237, Leu2185, Lys2187 |
| 51 | 3,4-F | -7.91 | 1.68 | 77 | Met2345, Val2240, Trp2239 | Trp2239, Met2345, Ile2356, Ile2237, Leu2185 |
| 55 | 3,4,5-F | -7.86 | 1.72 | 34 | Met2345, Val2240, Trp2239 | Met2345, Cys2243, Trp2239, Val2240, Leu2185, Ile2237, Ile2356 |
| 20 | 3-F, 4-CF3 | -7.85 | 1.76 | 87 | Met2345, Val2240, Trp2239 | Leu2185, Ile2237, Ile2356, Trp2239 |
| 28 | 2-F, 3-Cl, 6-CF3 | -7.81 | 1.89 | 38 | Glu2190, Tyr2225, Val2240, Gly2238, Tyr2225 | Lys2187, Ile2237, Ile2356, Leu2185, Cys2243, Val2240, Trp2239, Met2345 |
| 35 | 2,3,4,5,6-F | -7.81 | 1.89 | 97 | Tyr2225, Gly2238, Val2240, Trp2239 | Met2345, Trp2239, Cys2243, Leu2185, Tyr2225, Val2240 |
| 66 | 2,3,4,6-F | -7.79 | 1.96 | 87 | Gly2238, Val2240, Tyr2225 | Cys2243, Met2345, Trp2239, Tyr2225, Leu2185, Val2240 |
| 11 | 4-trifluoromethoxy | -7.77 | 2.02 | 67 | Phe2358, Asp2357 | Ile2356, Ile2237, Val2240, Cys2243, Met2345, Leu2354, Trp2239, Asp2195, Asp2357, Glu2190 |
| 19 | 2-F, 4-CF3 | -7.76 | 2.05 | 16 | Val2240, Gly2238, Tyr2225 | Ile2356, Trp2239, Leu2185, Ile2237 |

| NO | Substituen | FEB (kcal/mol) | KI (μM) | RUN | INTERACTION | |
|---|---|---|---|---|---|---|
| | | | | | HYDROGEN BOND | HYDROPHOBIC BOND |
| 16 | 2-F, 5-CF3 | -7.75 | 2.08 | 8 | Met2345, Cys2243, Trp2239, Val2240 | Trp2239, Val2240, Leu2185, Ile2237, Ile2356, Met2345 |
| 71 | 3-F, 4-OCH3 | -7.73 | 2.16 | 52 | Glu2190, Asp2195, Gly2238, Trp2239 | Leu2192, Leu2185, Ile2356, Ile2237, Met2345, Trp2239 |
| 53 | 2,4,5-F | -7.71 | 2.22 | 24 | Met2345, Val2240, Trp22239 | Cys2243, Leu2185, Ile2237, Ile2356, Met2345, Val2240, Trp2239\ |
| 5 | 3-CF3 | -7.7 | 2.28 | 52 | Trp2239, Val2240 | Leu2185, Ile2356, Ile2237, Met2345, Trp2239 |
| 23 | 2,4-CF3 | -7.64 | 2.52 | 99 | Asp2357, Cys2243, Val22240 | Leu2185, Ile2237, Ile2356, Cys2243, Val2240, Tyr2225, Leu2354, Met2345, Trp2239 |
| 65 | 2,3,4,5-F | -7.64 | 2.52 | 44 | Glu2190, Asp2195, Asp2244, Thr2245, Gly2238, Trp2239 | Ile2237, Trp2239, Cys2243, Met2345, Leu2185, Ile2356 |
| 9 | 3-OCF3 | -7.45 | 3.45 | 55 | Trp2239 | Met2345, Ile2356, Leu2185, Ile2237, Trp2239 |
| 15 | 3,5-CF3 | -7.25 | 4.85 | 47 | Trp2239, Asp2244, Thr2245 | Cys2243, Met2345, Trp2239, Ile2356, Ile2237, Leu2185 |
| | Native ligand | -9.67 | 0.08125 | 10 | Val2240, Tyr2225, Asp2195 | Met2345, Pro2169, Ile2163, Leu2185, Ile2237, Tyr2225, Ile2356, Trp2239, Val2240 |

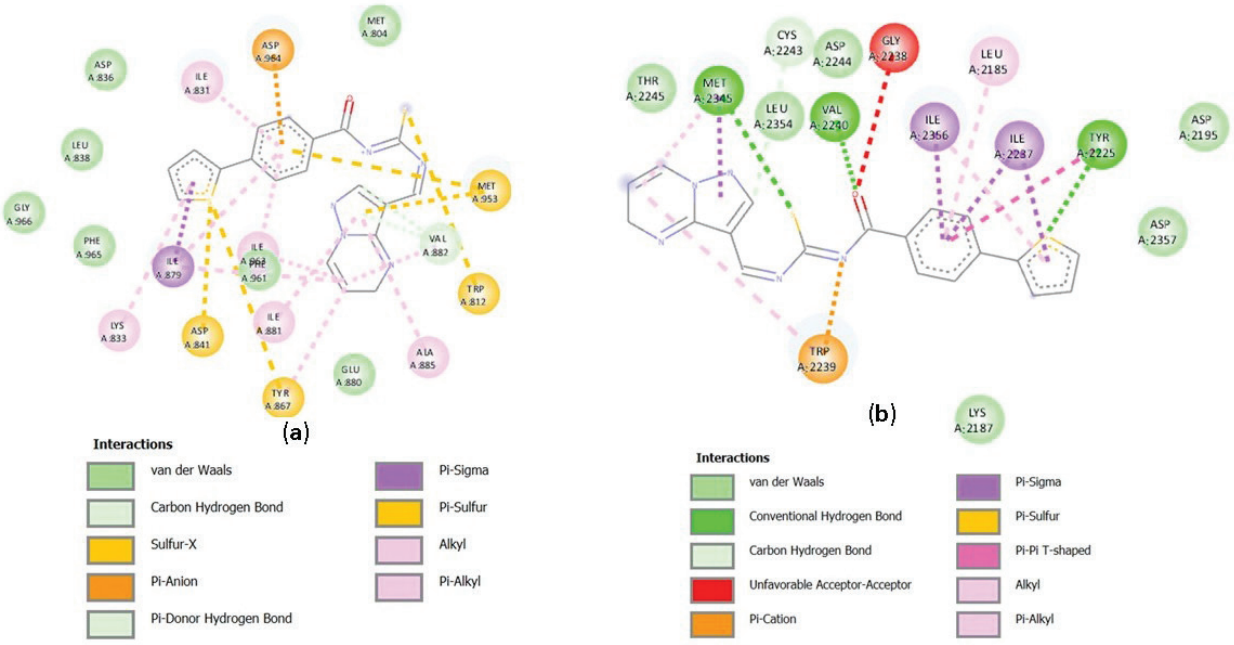


**Figure 4.** 2D visualization of compound 78 (4-thiophen) with PI3K (**a**) and mTOR (**b**).

interactions with natural ligands but also adds bond stabilization through additional interactions with polar and hydrophobic residues around the mTOR active site.

Docking results on both the PI3K and mTOR receptors show that several of the designed hybrid compounds have better binding affinities than natural ligands on both targets. At the PI3K receptor, the 2-phenylbenzoate compound recorded a free energy of binding (FEB) of –9.49 kcal/mol with an inhibition constant (Ki) of 0.111 μM, which is stronger than the natural ligand (FEB –8.09 kcal/mol; Ki 1.17 μM). This compound interacts with key residues such as Val882, Lys833, Asp964, Ile963, and Tyr867, which are also natural ligand-binding residues.

At the mTOR receptor, the compounds 4-phenyldiazen and 2-CN occupy the top positions, with FEB values of –10.07 kcal/mol (Ki 0.041–0.042 μM), surpassing natural ligands that have FEB values of –9.67 kcal/mol and Ki values of 0.081 μM. Dominant interactions occur at residues Asp2357, Cys2243, Val2240, Trp2239, and Tyr2225, which are part of the important mTOR binding pocket.

When compared across targets, it is apparent that several hybrid compounds (e.g., 2-phenylbenzoate, 4-thiadiazole, and 2-CN) are able to interact with key residues on both receptors, demonstrating a stable and consistent binding profile. The relatively small difference in affinity compared to natural ligands, which is even better in some cases, reinforces the indication that these compounds can be developed as dual PI3K/mTOR inhibitors.

Pharmacologically, the ability to target both proteins is highly relevant, given that the PI3K/Akt/mTOR pathway is a major axis in cancer cell proliferation, growth, and survival. Dual inhibition may increase therapeutic efficacy and reduce the possibility of resistance due to feedback loops when only one target is inhibited (Rodon et al. 2013; Fruman et al. 2017).

A deeper mechanistic interpretation indicates that the enhanced dual inhibitory potential of the thiourea–pyrazolopyrimidine hybrids is governed by their ability to establish persistent interactions with key catalytic and binding-site residues of both PI3K and mTOR. In the PI3K active site, the top-performing hybrids consistently interact with critical residues such as Val882, Lys833, Asp964, Tyr867, and Ile963, which are known to play important roles in ATP binding and ligand stabilization. Hydrogen bonding with Lys833 and Asp964, combined with hydrophobic and π–π interactions involving Tyr867 and surrounding hydrophobic residues, significantly contributes to the enhanced binding affinity. Similarly, within the mTOR binding pocket, strong and stable interactions are observed with residues Asp2357, Cys2243, Val2240, Trp2239, Tyr2225, and Ile2237, which are essential for ligand anchoring and catalytic function. Molecular dynamics simulations further confirm that these interactions are maintained over the simulation period, supporting a stable binding mode under dynamic conditions. Collectively, these residue-specific interactions provide a mechanistic explanation for the improved docking scores and stability of the hybrids, linking molecular recognition directly to their predicted dual PI3K/mTOR inhibitory potential.

## Molecular dynamic

The next step after molecular docking analysis is to perform molecular dynamics (MD) simulations to evaluate the stability of the ligand–receptor complex in greater depth. While docking only provides a static picture of affinity and binding modes, MD allows observation of the behavior of the complex under dynamic conditions that more closely resemble the biological environment. In this study, MD simulations were performed using Desmond software with a free academic license, which is known for its computational speed and energy calculation accuracy. Through the analysis of parameters such as root mean square deviation (RMSD), as shown in Figs 5, 7, root mean square fluctuation (RMSF), as shown in Figs 6, 8, radius of gyration, and the number of hydrogen bonds throughout the simulation time, the stability of the structure, the flexibility of the residues, and the consistency of ligand interaction with the active site can be assessed. This stage is very important for validating the docking results because only compounds with stable interactions within the simulation time frame are worth considering as potential PI3K/mTOR inhibitor candidates.

Molecular dynamics simulations were performed on several predicted compounds that showed good stability in the molecular docking process on both the PI3K receptor and the mTOR receptor compared to natural ligands, namely Compound-38, Compound-59, and Compound-78, with a simulation time of 30 ns.

The results of molecular dynamics (MD) simulations for 30 ns on the PI3K complex (3L54.pdb) show that the system with the native ligand is relatively the most stable, with an average RMSD value in the range of 1.5–2.0 Å, indicating that the complex structure is fairly consistent throughout the simulation. In contrast, complexes with hybrid compounds Compound-38, Compound-59, and Compound-78 showed higher RMSD values, around 2.5–3.5 Å, with more pronounced fluctuations at the beginning of the simulation before reaching stability after ~10 ns. Nevertheless, all RMSD values remained below 4 Å, thus qualifying as stable for protein–ligand systems (Kufareva and Abagyan 2012).

RMSF analysis shows that residues around the binding site remain stable, with low fluctuations (< 2 Å), both for the native ligand and the hybrid compounds, indicating

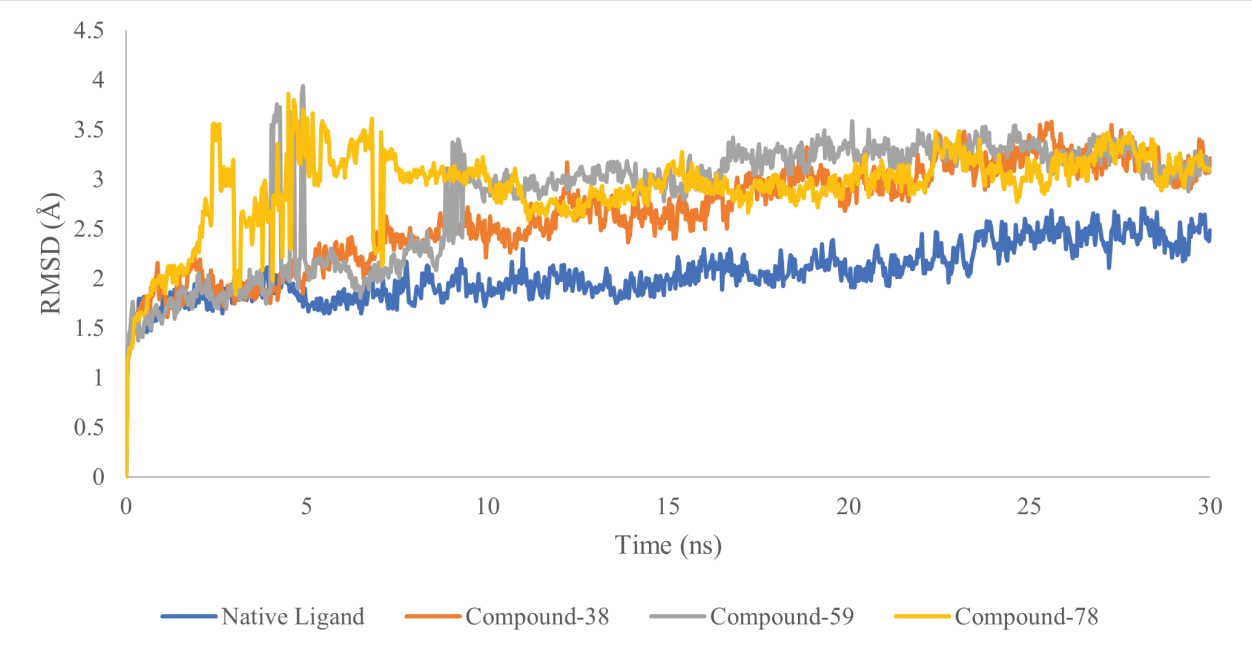


**Figure 5.** RMSD graph of the simulated compound–receptor PI3K (3L54.pdb) system over 30 ns.

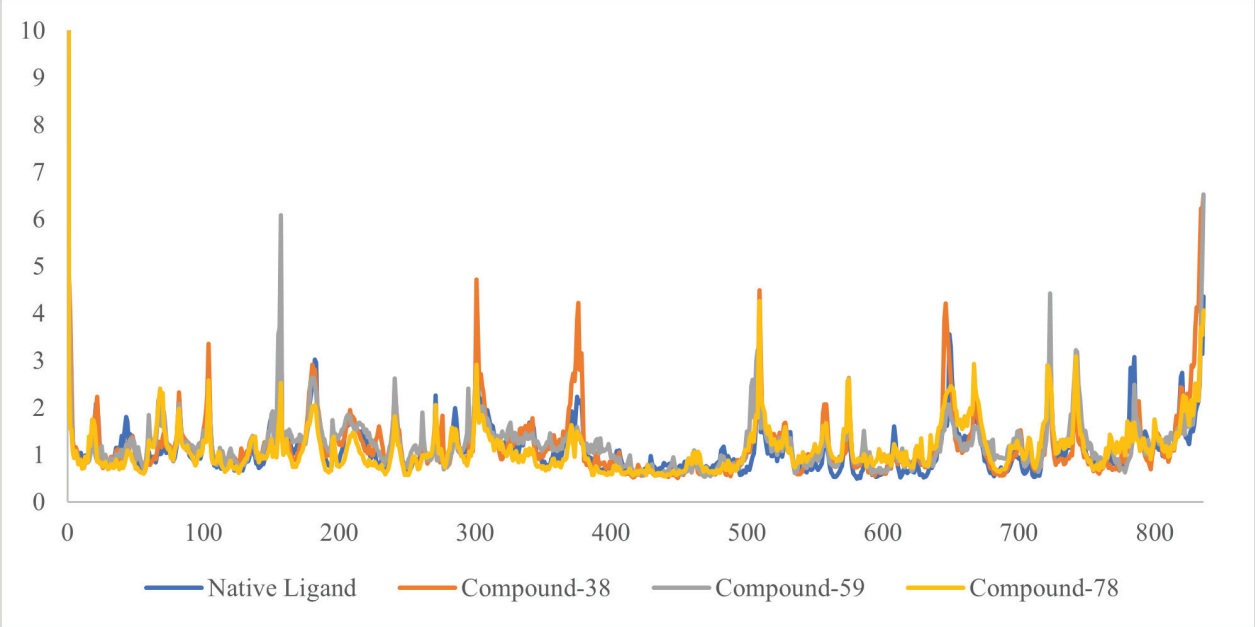


**Figure 6.** RMSF graph of the simulated compound–receptor PI3K (3L54.pdb) system over 30 ns.

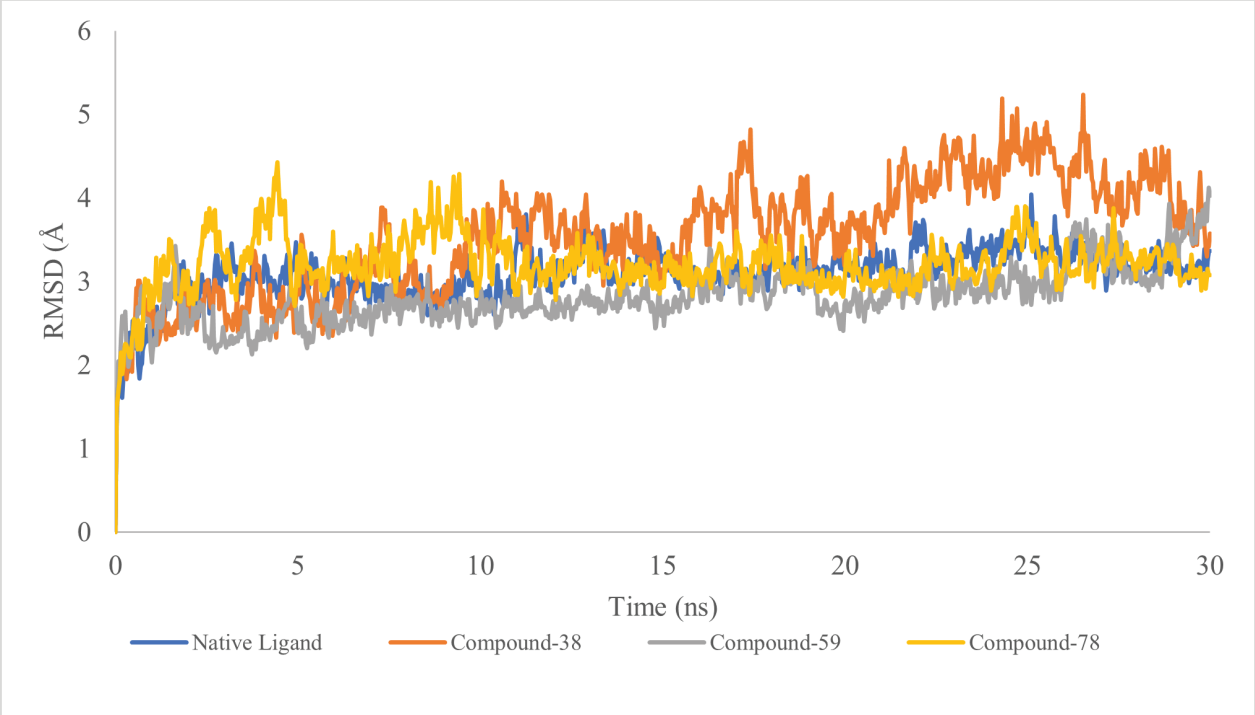


**Figure 7.** RMSD graph of the simulated compound–receptor mTOR (4JT6.pdb) system over 30 ns.

that ligand interactions with key residues are maintained. Higher fluctuations (up to 6–9 Å) occur only in the loop and terminal regions of the protein, which are naturally the most flexible parts. The complex with Compound-78 shows a slight increase in fluctuations in some segments compared to the natural ligand, but this does not interfere with the stability of the main interactions. Overall, the RMSD and RMSF results confirm that although the native ligand shows the highest stability, the hybrid compounds also form stable complexes and can be considered potential PI3K inhibitor candidates (Hollingsworth and Dror 2018).

The results of molecular dynamics (MD) simulations for 30 ns on the mTOR receptor complex (4JT6.pdb) show differences in stability between ligands based on RMSD and RMSF analyses. The RMSD graph shows that the complexes with the native ligand and Compound-59 and Compound-78 are relatively stable, with average deviations in the range of 2.0–3.0 Å, which is still within acceptable limits for protein–ligand systems. In contrast, Compound-38 showed greater fluctuations, reaching 4–5 Å in several simulation intervals, indicating that the conformation of this complex tends to be more dynamic and

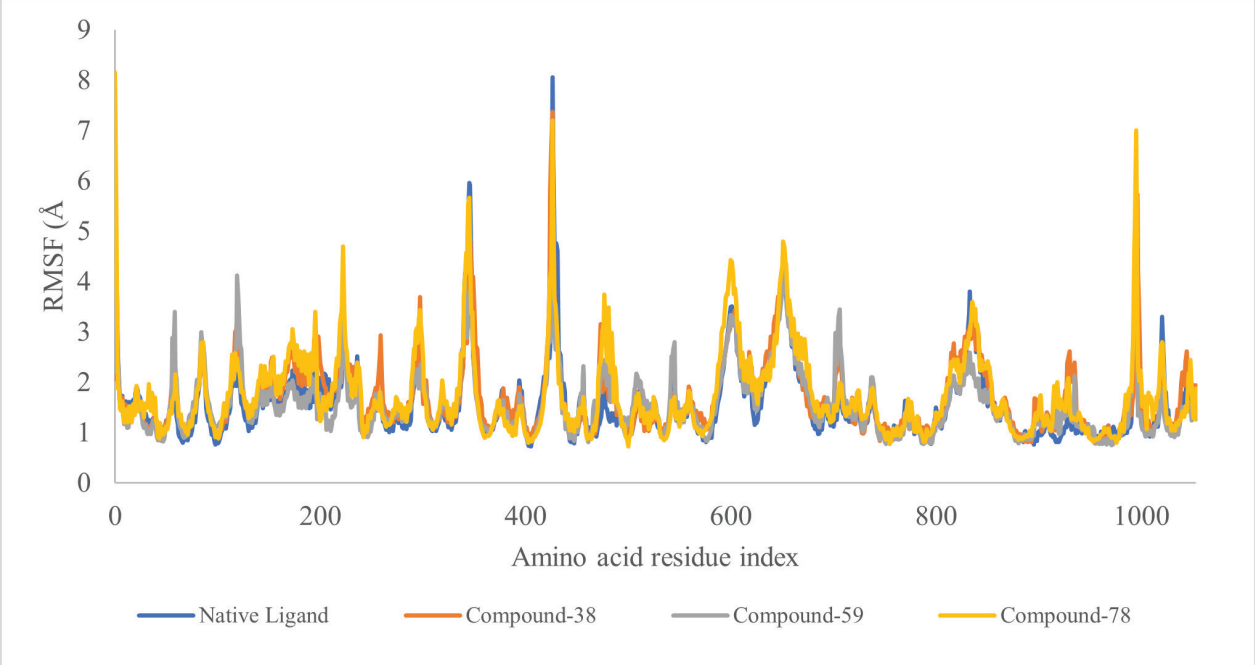


**Figure 8.** RMSF graph of the simulated compound–receptor mTOR system over 30 ns.

less stable than those of other ligands. In general, RMSD values that remain below 5 Å indicate that the overall complex is still stable, although complexes with the native ligand and Compound-59 are more consistent in maintaining structural stability throughout the simulation time (Kufareva and Abagyan 2012).

RMSF analysis shows that most residues in the protein–ligand complexes have low fluctuations (< 2 Å), especially in the region around the binding site, indicating that ligand interactions with key residues are well maintained. Higher fluctuation peaks (5–8 Å) occur only in the loop and terminal regions of the protein, which are naturally flexible. The complex with Compound-78 exhibits an RMSF pattern close to that of the native ligand, while Compound-38 shows a slight increase in fluctuations in several non-critical residues. This indicates that, although all complexes are stable, the native ligand and Compound-59 have the best dynamic profiles, while Compound-78 is also quite promising, with stability close to that of the natural ligand.

The combination of RMSD and RMSF data confirms that certain hybrid compounds, particularly Compound-59 and Compound-78, are able to maintain interaction stability with mTOR at levels comparable to the natural ligand. This reinforces the potential of hybrid compounds as competitive mTOR inhibitors and warrants further investigation in the context of dual PI3K/mTOR inhibitors (Hollingsworth and Dror 2018).

The stability of the Compound-78 interaction with the mTOR receptor in the molecular dynamics simulation is also supported by the interaction patterns observed between Compound-78 and the mTOR receptor, as shown in Figs 9, 10.

Fig. 9 shows the interaction profile of Compound-78 with the mTOR receptor during a 30 ns MD simulation, including hydrogen bonds, hydrophobic interactions, water bridges, and ionic interactions. Key residues such as Val2240, Cys2243, Asp2244, and Thr2245 contribute dominantly to maintaining the stability of the complex through both hydrogen bonding and hydrophobic interactions. In addition, aromatic residues such as Trp2239 and Tyr2225 play important roles through consistent hydrophobic interactions, while polar residues such as Asp2357 and Arg2247 form water bridges that further stabilize the system. This interaction pattern indicates that Compound-78 is able to maintain strong and repeated contact with critical residues in the mTOR active site, reinforcing its potential as an effective mTOR inhibitor. These results are consistent with the literature, which states that the combination of hydrophobic and hydrogen bonding interactions with key residues in the mTOR active domain is an important factor in supporting ligand–receptor affinity and stability (Hollingsworth and Dror 2018; Zhang et al. 2020).

Fig. 10 shows a timeline representation of Compound-78 interaction with the mTOR receptor during a 30 ns MD simulation. The top graph shows a relatively stable total number of contacts in the range of 6–10 interactions throughout the simulation time, indicating that the ligand is able to maintain consistent interactions with key residues. A detailed analysis at the bottom shows that the residues Trp2239, Val2240, Cys2243, Asp2244, and Thr2245 dominate the interactions through both hydrogen bonding and hydrophobic interactions, with high intensity throughout the simulation. In addition, polar residues such as Asp2357 and Arg2247 also play an important role in maintaining the stability of the complex through persistent water bridge interactions. This pattern confirms that Compound-78 is not only capable of forming strong interactions at the beginning of the simulation but also of

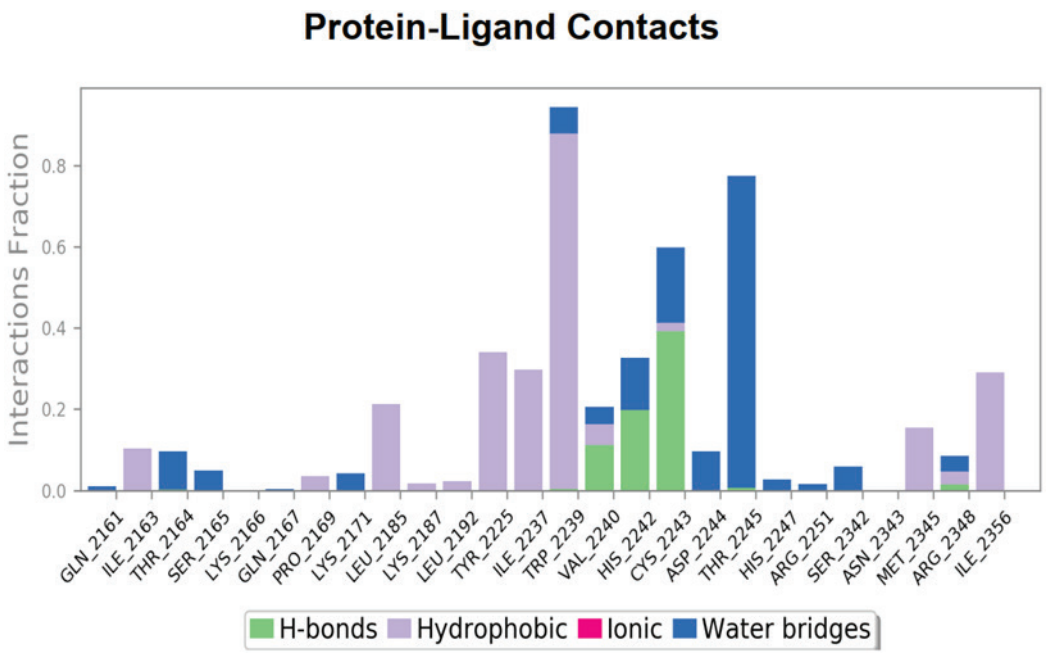


**Figure 9.** Protein–ligand contacts of compound 78 with the mTOR receptor during a 30 ns MD simulation.

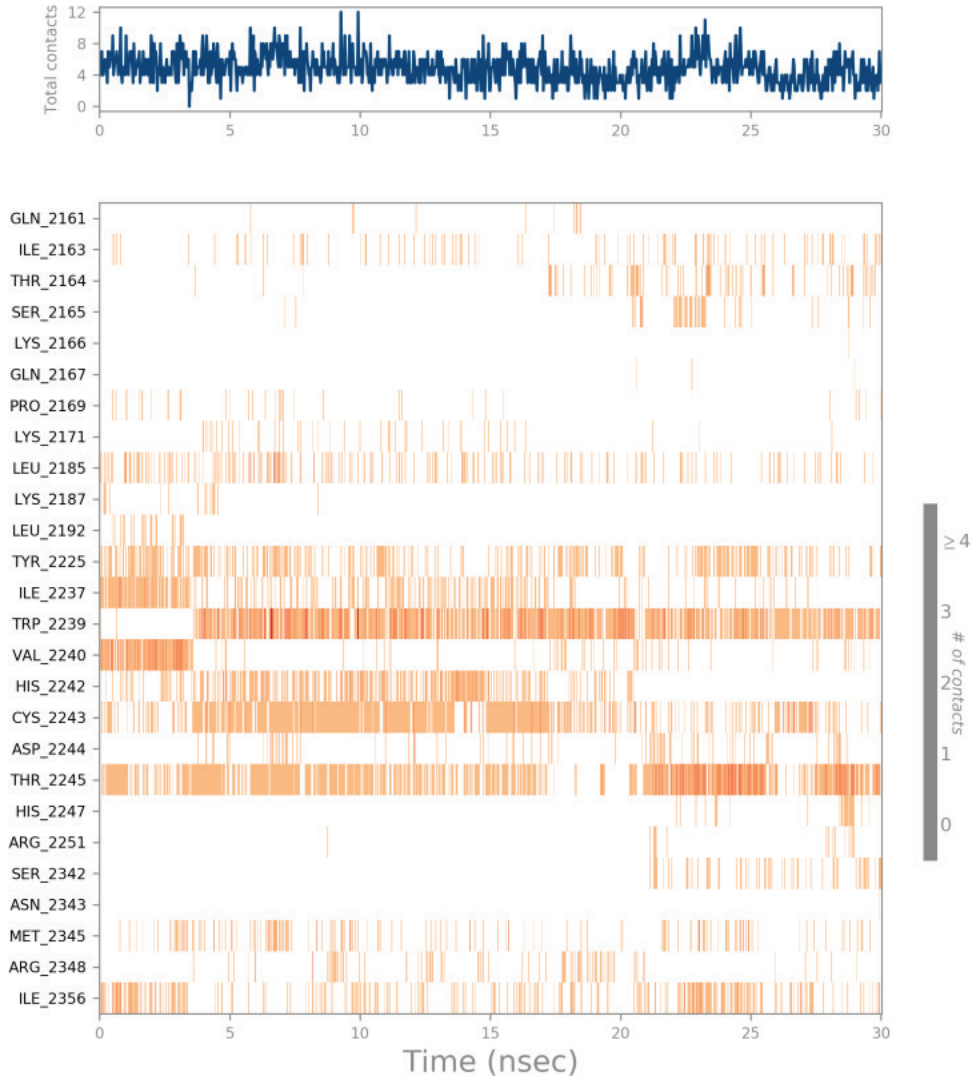


**Figure 10.** Timeline representation of the interactions and contacts of compound 78 with the mTOR receptor during a 30 ns MD simulation.

maintaining them continuously until the end, indicating bond stability and high potential as an mTOR inhibitor (Hollingsworth and Dror 2018).

Fig. 11 shows the analysis of the properties of the Compound-78 ligand in complex with the mTOR receptor during a 30 ns MD simulation. The RMSD parameter of the ligand is stable in the range of 1.0–2.0 Å, indicating that the ligand conformation is relatively maintained throughout the simulation. The radius of gyration (rGyr) value is consistent at approximately 4.0–4.5 Å, indicating that the ligand does not undergo major changes in structural compaction. The intra-HB pattern shows intermittent intramolecular hydrogen bond formation, which may support the stability of ligand orientation within the active site. Molecular surface area (MolSA) and solvent-accessible surface area (SASA) analyses show moderate fluctuations, indicating ligand adaptation to the receptor and solvent environment. Meanwhile, the polar surface area (PSA) value tends to be stable in the range of 85–95 Å$^2$, consistent with the ligand maintaining optimal polarity to interact with mTOR active residues. Overall, these results confirm that Compound-78 is able to maintain structural stability and strong interactions with mTOR, supporting its potential as an effective inhibitor (Hollingsworth and Dror 2018).

To strengthen the comparative assessment, a quantitative evaluation of the top-performing hybrid compounds was conducted against the reference ligands used in the PI3K and mTOR crystal structures. The leading hybrids exhibited more favorable binding free energy (ΔG) values and lower predicted inhibition constants (Ki) than the native ligands, indicating enhanced inhibitory potential. In addition, molecular dynamics analyses revealed comparable or improved complex stability for the selected hybrids, as reflected by consistent RMSD and RMSF profiles and sustained hydrogen bond occupancy throughout the simulation period. These quantitative comparisons provide clearer evidence that the proposed thiourea–pyrazolopyrimidine hybrids can outperform known inhibitors at the molecular interaction level.

## Conclusion

This study successfully designed and evaluated thiourea–pyrazolopyrimidine hybrid compounds as potential dual PI3K/mTOR inhibitors using a comprehensive *in silico* approach. Molecular docking results revealed that several derivatives, particularly those with 2-phenylbenzoate and 4-thiophen substituents, exhibited stronger binding affinities than native ligands, with stable interactions at key residues of PI3K and mTOR. Validation through 30 ns molecular dynamics simulations confirmed the stability of the ligand–receptor complexes, as indicated by consistent RMSD and RMSF values. Pharmacokinetic and toxicity predictions demonstrated that most compounds showed good absorption profiles, high oral bioavailability, and lower toxicity potential compared to the lead compound. Overall, these findings emphasize that the designed hybrid compounds show strong promise as novel anticancer agents with dual inhibitory mechanisms against PI3K/mTOR, warranting further development through advanced synthesis and subsequent *in vitro* and *in vivo* biological evaluations.

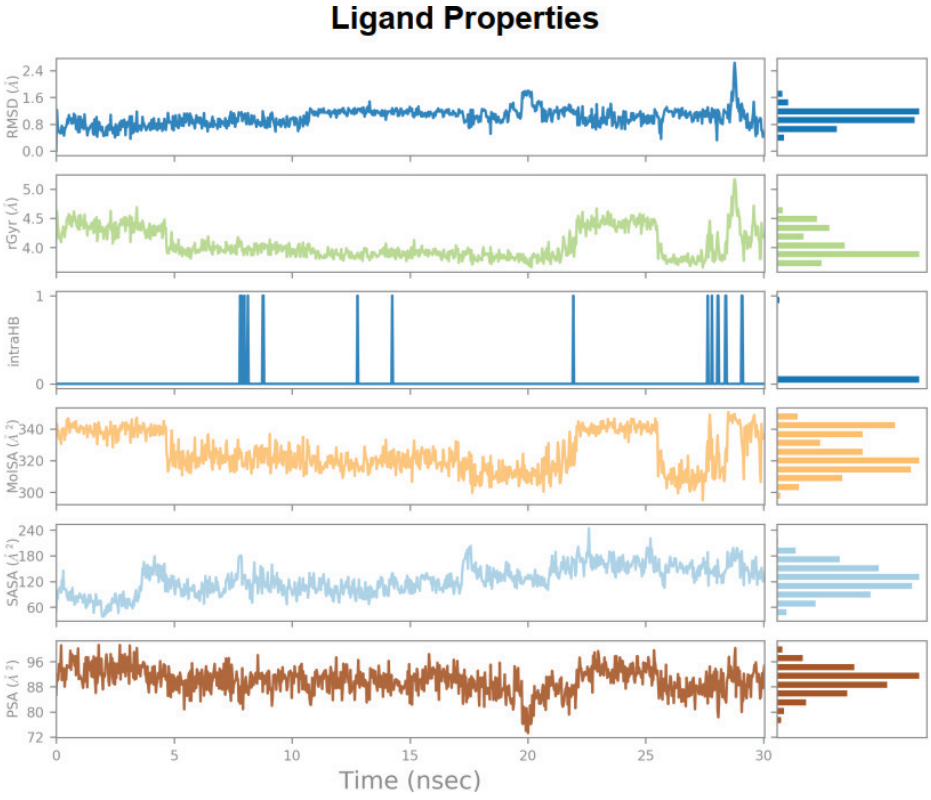


**Figure 11.** Analysis of ligand properties of compound 78 in complex with mTOR during a 30 ns MD simulation.

## Acknowledgements

The authors gratefully acknowledge the Research Centre for Pharmaceutical Ingredients and Traditional Medicine, National Research and Innovation Agency (BRIN), for supporting these research activities.

## Additional information

### Conflict of interest

The authors have declared that no competing interests exist.

### Ethical statements

The authors declared that no clinical trials were conducted in the present study.

The authors declared that no experiments on humans or human tissues were performed in the present study.

The authors declared that no informed consent was obtained from the humans, donors or donors' representatives participating in the study.

The authors declared that no experiments on animals were performed for the present study.

The authors declared that no commercially available immortalised human and animal cell lines were used in the present study.

### Use of AI

No use of AI was reported.

### Funding

This research was funded by the Ministry of Higher Education, Science, and Technology of Indonesia in 2025 (Grant Nos. 125/C3/DT.05.00/PL.2025 and 8026/LL4/PG/2025).

### Author contributions

All authors have contributed equally.

### Author ORCIDs

Ruswanto Ruswanto https://orcid.org/0000-0003-2580-266X
Tita Nofianti https://orcid.org/0009-0000-7542-3807
Richa Mardaningrum https://orcid.org/0000-0002-2327-363X
Dini Kesuma https://orcid.org/0000-0002-6612-372X
Sofa Fajriah https://orcid.org/0000-0002-1758-2102

### Data availability

All of the data that support the findings of this study are available in the main text.

## References

Colovos C, Yeates TO (1993) Verification of protein structures: patterns of nonbonded atomic interactions. Protein Science 2: 1511–1519. https://doi.org/10.1002/pro.5560020916

Fruman DA, Chiu H, Hopkins BD, Bagrodia S, Cantley LC, Abraham RT (2017) The PI3K pathway in human disease. Cell 170: 605–635. https://doi.org/10.1016/j.cell.2017.07.029

Gao H, Li Z, Wang K, Zhang Y, Wang T, Wang F, Xu Y (2023) Design, synthesis, and biological evaluation of sulfonamide methoxypyridine derivatives as novel PI3K/mTOR dual inhibitors. Pharmaceuticals 16: 461. https://doi.org/10.3390/ph16030461

Gontijo VS, Viegas FPD, Ortiz CJC, de Freitas Silva M, Damasio CM, Rosa MC, Campos TG, Couto DS, Tranches Dias KS, Viegas C (2020) Molecular hybridization as a tool in the design of multi-target directed drug candidates for neurodegenerative diseases. Current Neuropharmacology 18: 348–407. https://doi.org/10.2174/1385272823666191021124443

Guengerich FP (2011) Mechanisms of drug toxicity and relevance to pharmaceutical development. Drug Metabolism and Pharmacokinetics 26: 3–14. https://doi.org/10.2133/dmpk.DMPK-10-RV-062

Hollingsworth SA, Dror RO (2018) Molecular dynamics simulation for all. Neuron 99: 1129–1143. https://doi.org/10.1016/j.neuron.2018.08.011

Huang M, Duan W, Chen N, Lin G, Wang X (2022) Synthesis and antitumor evaluation of menthone-derived pyrimidine-urea compounds as potential PI3K/Akt/mTOR signaling pathway inhibitor. Frontiers in Chemistry 9: 815531. https://doi.org/10.3389/fchem.2021.815531

Jain S, Gupta SP (2023) Molecular design and docking study of novel quinoxaline-containing compounds as PI3K/mTOR dual inhibitor. International Journal of Pharmaceutical Sciences and Research 14: 4513–4523.

Janku F, Yap TA, Meric-Bernstam F (2018) Targeting the PI3K pathway in cancer: are we making headway? Nature reviews Clinical oncology 15: 273–291. https://doi.org/10.1038/nrclinonc.2018.28

Kazius J, McGuire R, Bursi R (2005) Derivation and validation of toxicophores for mutagenicity prediction. Journal of medicinal chemistry 48: 312–320. https://doi.org/10.1021/jm040835a

Kucuksayan E, Ozben T (2017) Hybrid compounds as multitarget directed anticancer agents. Current Topics in Medicinal Chemistry 17: 907–918. https://doi.org/10.2174/1568026616666160927155515

Kufareva I, Abagyan R (2012) Methods of protein structure comparison. In: Homology modeling: Methods and protocols. Springer, 231–257. https://doi.org/10.1007/978-1-61779-588-6_10

Lee W, Ortwine DF, Bergeron P, Lau K, Lin L, Malek S, Nonomiya J, Pei Z, Robarge KD, Schmidt S, Others (2013) A hit to lead discovery of novel N-methylated imidazolo-, pyrrolo-, and pyrazolo-pyrimidines as potent and selective mTOR inhibitors. Bioorganic & Medicinal Chemistry Letters 23: 5097–5104. https://doi.org/10.1016/j.bmcl.2013.07.027

Mardianingrum R, Endah SRN, Suhardiana E, Ruswanto R, Siswandono S (2021) Docking and molecular dynamic study of isoniazid derivatives as anti-tuberculosis drug candidate. Chemical Data Collections 32: 100647. https://doi.org/10.1016/j.cdc.2021.100647

Mortelmans K, Zeiger E (2000) The Ames Salmonella/microsome mutagenicity assay. Mutation Research – Fundamental and Molecular Mechanisms of Mutagenesis 455: 29–60. https://doi.org/10.1016/S0027-5107(00)00064-6

Pires DE, Blundell TL, Ascher DB (2015) pkCSM: predicting small-molecule pharmacokinetic and toxicity properties using graph-based signatures. Journal of Medicinal Chemistry 58: 4066–4072. https://doi.org/10.1021/acs.jmedchem.5b00104

Porta C, Paglino C, Mosca A (2014) Targeting PI3K/Akt/mTOR signaling in cancer. Frontiers in Oncology 4: 64. https://doi.org/10.3389/fonc.2014.00064

Purser S, Moore PR, Swallow S, Gouverneur V (2008) Fluorine in medicinal chemistry. Chemical Society Reviews 37: 320–330. https://doi.org/10.1039/B610213C

Ramachandran GN, Ramakrishnan C, Sasisekharan V (1963) Stereochemistry of polypeptide chain configurations. Journal of Molecular Biology 7: 95–99. https://doi.org/10.1016/S0022-2836(63)80023-6

Renadi S, Pratita ATK, Mardianingrum R, Ruswanto R (2023) The potency of alkaloid derivates as anti-breast cancer candidates: *In silico* Study. Jurnal Kimia Valensi 9: 89–108. https://doi.org/10.15408/jkv.v9i1.31481

Rodon J, Dienstmann R, Serra V, Tabernero J (2013) Development of PI3K inhibitors: lessons learned from early clinical trials. Nature Reviews Clinical Oncology 10: 143–153. https://doi.org/10.1038/nrclinonc.2013.10

Ruswanto, Siswandono, Richa M, Tita N, Tresna L (2017) Molecular docking of 1-benzoyl-3-methylthiourea as anti cancer candidate and its absorption, distribution, and toxicity prediction. Journal of Pharmaceutical Sciences and Research 9: 680–684.

Ruswanto, Miftah AM, Tjahjono DH, Siswandono AMM (2015) Synthesis and *in vitro* Cytotoxicity of 1-Benzoyl-3-methyl thiourea Derivatives. Prochedia Chemistry 17: 157–161. https://doi.org/10.1016/j.proche.2015.12.105

Ruswanto R, Miftah AM, Tjahjono DH, Siswandono (2021) *In silico* study of 1-benzoyl-3-methylthiourea derivatives activity as epidermal growth factor receptor (EGFR) tyrosine kinase inhibitor candidates. Chemical Data Collections 34: 100741. https://doi.org/10.1016/j.cdc.2021.100741

Ruswanto R, Mardianingrum R, Lestari T, Nofianti T, Siswandono S (2018) 1-(4-Hexylbenzoyl)-3-methylthiourea. MolBank 2018: 2–6. https://doi.org/10.3390/M1005

Ruswanto R, Nofianti T, Mardianingrum R, Kesuma D, Siswandono (2022) Design, molecular docking, and molecular dynamics of thiourea-iron (III) metal complexes as NUDT5 inhibitors for breast cancer treatment. Heliyon: e10694. https://doi.org/10.1016/j.heliyon.2022.e10694

Ruswanto R, Mardianingrum R, Nofianti T, Fizriani R, Siswandono S (2023a) Computational Study of Bis-(1-(Benzoyl)-3-Methyl Thiourea) Platinum (II) Complex Derivatives as Anticancer Candidates. Advances and Applications in Bioinformatics and Chemistry 16: 15–36.

Ruswanto R, Mardianingrum R, Nofianti T, Pratita ATK, Naser FM, Siswandono S (2023b) Design and computational study of the thiourea–cobalt(III) complex as an anticancer candidate. Journal of Pharmacy and Pharmacognosy Research 11: 499–516. https://doi.org/10.56499/jppres23.1622_11.3.499

Sabbah DA, Brattain MG, Zhong H (2011) Dual inhibitors of PI3K/mTOR or mTOR-selective inhibitors: which way shall we go? Current Medicinal Chemistry 18: 5528–5544. https://doi.org/10.2174/092986711798347298

Septian AD, Wardani GA, Mardianingrum R, Ruswanto R (2023) The virtual screening of flavonoid derivatives on progesterone, estrogen, and HER-2 receptor for breast cancer treatment candidate. Jurnal Kimia Valensi 9: 163–182. https://doi.org/10.15408/jkv.v9i1.31482

Siegel RL, Miller KD, Wagle NS, Jemal A (2023) Cancer statistics, 2023. CA: a Cancer Journal for Clinicians 73: 17–48. https://doi.org/10.3322/caac.21763

Silalahi R, Pratita AT, Ruswanto R (2025) Potential of garlic (*Allium sativum* L.) compounds as antibreastcancer candidates: Computational Study. Tropical Journal of Natural Product Research 9. https://doi.org/10.26538/tjnpr/v9i4.21

Szumilak M, Wiktorowska-Owczarek A, Stanczak A (2021) Hybrid drugs—a strategy for overcoming anticancer drug resistance? Molecules 26: 2601. https://doi.org/10.3390/molecules26092601

Wang Y, Tortorella M (2022) Molecular design of dual inhibitors of PI3K and potential molecular target of cancer for its treatment: A review. European Journal of Medicinal Chemistry 228: 114039. https://doi.org/10.1016/j.ejmech.2021.114039

Welker ME, Kulik G (2013) Recent syntheses of PI3K/Akt/mTOR signaling pathway inhibitors. Bioorganic & Medicinal Chemistry 21: 4063–4091. https://doi.org/10.1016/j.bmc.2013.04.083

Zhang Y, Meng X, Tang H, Cheng M, Yang F, Xu W (2020) Design, synthesis, and biological evaluation of novel substituted thiourea derivatives as potential anticancer agents for NSCLC by blocking K-Ras protein-effectors interactions. Journal of Enzyme Inhibition and Medicinal Chemistry 35: 344–353. https://doi.org/10.1080/14756366.2019.1702653